Behavioral/Systems/Cognitive

Neural Circuitry of Stress-Induced Insomnia in Rats

Georgina Cano, Takatoshi Mochizuki, and Clifford B. Saper

Department of Neurology, Beth Israel Deaconess Medical Center, Division of Sleep Medicine and Program in Neuroscience, Harvard Medical School, Boston, Massachusetts 02215

Sleep architecture is often disturbed after a stressful event; nevertheless, little is known about the brain circuitry responsible for the sleep perturbations induced by stress. We exposed rats to a psychological stressor (cage exchange) that initially causes an acute stress response, but several hours later generates a pattern of sleep disturbances similar to that observed in stress-induced insomnia in humans: increased sleep latency, decreased non-REM (nREM) and REM sleep, increased fragmentation, and high-frequency EEG activity during nREM sleep. We examined the pattern of Fos expression to identify the brain circuitry activated, and found increased Fos in the cerebral cortex, limbic system, and parts of the arousal and autonomic systems. Surprisingly, there was simultaneous activation of the sleep-promoting areas, most likely driven by ongoing circadian and homeostatic pressure. The activity in the cerebral cortex and arousal system while sleeping generates a novel intermediate state characterized by EEG high-frequency activity, distinctive of waking, during nREM sleep. Inactivation of discrete limbic and arousal regions allowed the recovery of specific sleep components and altered the Fos pattern, suggesting a hierarchical organization of limbic areas that in turn activate the arousal system and subsequently the cerebral cortex, generating the high-frequency activity. This high-frequency activity during nREM was eliminated in the stressed rats after inactivating parts of the arousal system. These results suggest that shutting down the residual activity of the limbic-arousal system might be a better approach to treat stress-induced insomnia, rather than potentiation of the sleep system, which remains fully active.

Key words: **stress; sleep disturbances; insomnia; rat model; Fos; arousal system; limbic system**

Introduction

Stress has a significant impact on sleep–wake behavior in all animals. The immediate effect of exposure to a stressor is increased wakefulness and arousal, as an adaptive response to ensure survival by fully reacting to a potentially harmful stimulus. Nevertheless, the effects of stress on sleep in experimental studies vary significantly depending on the stress paradigm, when it is applied (dark or light phase), duration (acute vs chronic), strains of rats or mice, and the individual vulnerability to stress (high- or low-responding animals). For a detailed review of models of stress-induced sleep disturbances in rodents, see Pawlyk et al. (2008).

Some human disorders associated with stress or dysregulation of the stress system, such as anxiety and major depression (Arborelius et al., 1999), also cause secondary sleep perturbations. In other cases, the stress-induced sleep perturbation is a primary component of the pathological condition, as in posttraumatic stress disorder (PTSD) (Ross et al., 1989) or primary insomnia (not caused by psychiatric or medical conditions, pain, or substance abuse) (Nowell et al., 1997; Vgontzas and Kales, 1999). Primary insomnia, which is often precipitated by stressful life events in predisposed individuals, occurs in 25% of all chronic insomnia patients (Roth and Roehrs, 2003), whereas occasional or transient insomnia associated with stress is extremely common in the adult population, estimates ranging from 25–35% (Sarrais and de Castro-Manglano, 2007) to 80% (Pagel and Parnes, 2001).

Although the sleep perturbations induced by stress have deleterious effects on health, little is known about the neural circuitry underlying it. A key problem in generating an animal model of stress-induced insomnia is that most ongoing acute stressors produce continual wakefulness (sleep deprivation), with a pattern of neuronal activity characteristic of the waking circuitry. After cessation of the stressor, there is usually a sleep rebound in response to the previous sleep deprivation, and the pattern of brain activity is the typical sleeping pattern. Neither pattern adequately models the sleep perturbations seen in human stress-induced insomnia, in which the typical stressor is a self-sustaining psychological state rather than a continued external intervention. We have developed a rat model using a species-specific psychological stressor that causes an initial acute stress response, as indicated by "freezing" behavior and increased neuronal activation (Fos) of the medial parvicellular paraventricular hypothalamic nucleus (mpPVH). However, several hours later, when these indicators of acute stress have waned, we observed a pattern of sleep disturbances similar to that reported during stress-induced insomnia in humans. We then examined the Fos expression in the brain to identify the circuitry activated during this period. In addition, we inhibited discrete regions of the circuitry (cell-specific lesions or pharmacological inhibition) to analyze the recovery of specific sleep parameters and the changes in Fos expression. These data suggest the existence of a hierarchical network of neuronal groups responsible for the sleep distur-

Received April 24, 2008; revised July 16, 2008; accepted Aug. 13, 2008.

This work was supported by National Institutes of Health Grants HL07901 and MH-071106 (G.C.) and HL60292 and AG009975 (C.B.S.). We thank Dr. Michael L. Perlis (University of Rochester, Rochester, NY) for his insightful comments and discussions and Quan Ha for her excellent technical assistance.

Correspondence should be addressed to Clifford B. Saper, Department of Neurology, Beth Israel Deaconess Medical Center, 330 Brookline Avenue, Boston, MA 02215. E-mail: csaper@bidmc.harvard.edu.

DOI:10.1523/JNEUROSCI.1809-08.2008

 0270-6474/08/2810167-18$15.00/0

bances observed in our rats. This model might be considered an initial step toward a better understanding of brain activation during stress-induced insomnia, and might provide insights into the neural circuitry involved in insomnia in humans.

Materials and Methods

Rats. Adult male Sprague Dawley rats ($n = 79$; weight = 275–325 g) from Harlan were housed individually under a 12 h light/dark cycle (lights on at 7:00 A.M.) at 22°C, with *ad libitum* access to food and water. All procedures conformed to the regulations detailed in the National Institutes of Health *Guide for the Care and Use of Laboratory Animals* and were approved by the Institutional Animal Care and Use Committees of Beth Israel Deaconess Medical Center and Harvard Medical School.

Surgery (implants and lesions). Rats ($n = 59$) were anesthetized with intraperitoneal chloral hydrate (350 mg/kg). The skull was exposed, and four screw electrodes were implanted (two on each side). Two EMG electrodes were placed into the nuchal muscles. All electrodes were connected to a pedestal socket, which was fixed to the skull with dental cement. After 2 weeks of recovery, rats were connected to the recording apparatus during 3 d for habituation. To study the role of discrete brain regions on the pattern of sleep disturbances induced by stress, we placed cell-specific lesions in 24 rats before EEG/EMG implants. Rats were microinjected bilaterally with 10% ibotenic acid in the infralimbic cortex (IFC) [$n = 8$; 25 nl on anteroposterior (AP), +2.5 mm; dorsoventral (DV), −4.5 mm; right–left (RL), +0.6, −0.6 mm] or in both the central nucleus of the amygdala (CeA) and the bed nucleus of the stria terminalis (BST) ($n = 8$; 15 nl on AP, −2.6 mm; DV, −6.8 mm; RL, +4.1, −4.1 mm for the CeA; 10 nl on AP, −0.3 mm; DV, −6.0 mm; RL, +1.5, −1.5 mm for the BST). We lesioned both the CeA and BST in the same animals because these two nuclei are tightly reciprocally interconnected, contain the same neurotransmitters, have similar functions, target similar brain regions, and receive analogous afferent innervation (Moga et al., 1989; Alheid et al., 1998; Dong et al., 2001); thus it is thought that they represent a single structure, the extended amygdala, which over the course of evolution became split into two groups at either end of the stria terminalis (Moga et al., 1989). In preliminary experiments, we found that only lesions that eliminated Fos expression at both sites, CeA and BST, were effective in restoring sleep. The locus ceruleus (LC) was lesioned by injecting 8 μl of 6% 6-OH-dopamine in the fourth ventricle (AP, −7.6 mm; DV, −4.5 mm; RL, 0.0 mm). All coordinates are from the rat brain atlas by Paxinos and Watson (1998). After lesions, rats were implanted for EEG/EMG as described above.

To determine the extent of neuronal loss, we counted Nissl-stained neurons with identifiable nuclei in two sections separated by 175 μm, bilaterally, in control rats and in rats with lesions in the IFC and CeA–BST. Nissl-stained neurons were counted in a 416 × 416 μm box placed at the lower tip of the forceps minor and dorsal to the dorsal peduncular cortex to count neurons in the IFC. For the CeA, the box was centered in the middle of the nucleus. Neurons in the BST were counted by placing the box between the upper edge of the anterior commissure and the ventral surface of the lateral ventricle. The extent of neuronal loss in the LC was determined by counting the remaining noradrenergic neurons in the whole extent of the nucleus in a 1:5 set of sections labeled with mouse anti-dopamine β-hydroxylase (1:10,000). In each case, we only counted neurons that had a clear nucleus. We measured the nuclear diameters in a sample of 25 neurons from each group and corrected the cell counts for nuclear size by using the Abercrombie correction factor.

Stress-induced sleep perturbations. After recording baseline EEG/EMG for 48 h, rats ($n = 16$) were placed at 10:00 A.M. into a dirty cage previously occupied by another male rat for 1 week (cage exchange). Rats were left undisturbed in the dirty cage until they were killed at 3:30 P.M. Control rats ($n = 9$) were placed in a clean cage at the same time to synchronize the ultradian cycles of both groups. To examine the brain circuitry involved in stress-induced acute insomnia, we killed the rats at 3:30 P.M., ~90 min after the onset of this sleep-disturbed period (5.5 h after cage exchange). We chose this time because animals show sleep fragmentation and decreased sleep beginning ~4 h after cage exchange, and 90 min is the optimal time to detect Fos expression associated with a specific stimulus. In addition to the clean cage controls, four additional groups were included: four rats were left to sleep undisturbed and killed at 6:50 P.M., at a time of the day when they had spontaneously been awake ~50% of the time during the preceding 90 min. A group of five rats was transferred to a dirty cage at 10:00 A.M. and killed 90 min after cage exchange to examine the pattern of Fos corresponding to the initial stress response. Two rats were transferred to a clean cage at 10:00 A.M. and killed 90 min after for comparison with the previous group. An additional group of four rats was killed at 9:00 P.M., when the animals were spontaneously awake (peak of activity).

After recording baseline EEG/EMG for 48 h, rats with brain lesions in the IFC, CeA–BST, or LC were also placed in dirty cages at 10:00 A.M. and killed at 3:30 P.M., similar to cage exchange rats. Neurons in the tuberomammillary nucleus (TMN) are resistant to ibotenic acid; therefore, to study the role of the TMN on stress-induced sleep perturbations, we injected immepip (10 mg/kg, i.p.), an H3 agonist that binds to inhibitory autoreceptors in the TMN (Jansen et al., 1998), immediately before cage exchange in six rats implanted with EEG/EMG. The rest of the procedure was similar to that performed for the other groups.

Sleep analysis. The EEG/EMG signals were amplified using a Grass polygraph and digitized using the ICELUS program (G Systems). The EEG filtering settings were 0.3 and 100 Hz for low and high cutoff, respectively, with the presence of a 60 Hz notch filter. Wake–sleep states were scored manually in 12 s epochs based on the digitized EEG/EMG. Wakefulness was identified by the presence of desynchronized EEG and high EMG activity. Non-REM (nREM) sleep was identified by the presence of a high-amplitude slow-wave EEG and low levels of EMG activity relative to waking. REM sleep was characterized by the presence of regular theta activity coupled with very low EMG tone compared with nREM sleep. For all experimental groups, the percentage of time spent in wake, nREM, and REM sleep and the number of bouts in each state were determined for each hour during baseline (BL) and experimental day (ExpDay) from 7:00 A.M. to 3:30 P.M. The sleep latency was calculated as the number of minutes from cage exchange to the first nREM bout.

To determine whether the lesions might alter the normal sleep–wake cycle, we analyzed 24 h of wake–sleep behavior 2 d before the cage exchange in lesioned rats from each group and compared with the baseline of nonlesioned rats (clean cage and cage exchange groups) at the same period.

Selected recordings from the BL and the ExpDay for clean cage, cage exchange, LC lesion, and immepip treatment groups were imported into SleepSign software (Kissei Comtec). The interval from 2:00 to 3:30 P.M. in the BL and ExpDay was manually scored again using 4 s epochs. To assess the possibility of microfragmentation during stress-induced acute insomnia, the number and mean duration of microbouts (wake, nREM, and REM) were calculated for both groups in the ExpDay. In addition, the EEG power spectrum during nREM sleep was obtained for the interval 2:00 to 3:30 P.M. in the BL and ExpDay, and the power ratio between the ExpDay and BL (ExpDay/BL × 100) was calculated for all frequencies at 0.25 Hz intervals in clean cage, cage exchange, LC lesions, and immepip treatment groups. The band spectrum used was that defined by Maloney et al. (1997) for rats: delta = 1.5–4; theta = 4.25–8.75; sigma = 9–14; beta = 14.25–30; and gamma = 30.25–58 Hz.

Temperature analysis. To assess whether the rats showed stress-induced hyperthermia during the cage exchange protocol, we analyzed the changes in temperature during the experimental day (from 7:00 A.M. to 4:00 P.M.) in nine rats implanted intraperitoneally with transmitters for temperature measurement (DSI System). Five rats were placed at 10:00 A.M. into dirty cages, whereas four rats were placed into clean cages. Baseline temperature was recorded previously during 24 h.

Immunohistochemistry. Rats were deeply anesthetized with chloral hydrate (500 mg/kg) and perfused transcardially with 100 ml of saline followed by 400 ml of 10% neutral phosphate-buffered formalin. Brains were removed and postfixed for 3 h in formalin and then transferred to 20% sucrose overnight. Brains were sectioned on a freezing microtome at 35 μm into five series. Sections were washed several times in 0.1 M PBS, pH 7.4, for 1 h, then incubated in 0.3% hydrogen peroxide in PBS containing 0.3% Triton X-100 (PBT), and washed again in PBS for 30 min. Sections were incubated in the primary antiserum in PBT for 24 h at

room temperature. Sections were rinsed in PBS and incubated in biotinylated secondary antibody in PBT for 1 h, rinsed three times in PBS, and incubated in avidin–biotin complex (Elite ABC; Vector Laboratories) for 1 h. After three rinses, sections were incubated in 1% diaminobenzidine (DAB), 0.05% nickel ammonium sulfate, and 0.05% cobalt chloride, and reacted with 0.01% hydrogen peroxide to obtain a black nuclear precipitate for Fos detection, or incubated in DAB with hydrogen peroxide to determine the neuronal phenotype (brown stained cytoplasm). Sections were washed, mounted on gelatin-coated glass slides, dehydrated in graded alcohols, cleared in xylene, and coverslipped.

To detect and quantify Fos expression, a 1:5 series of sections was incubated in primary antiserum against Fos (1:25,000). To detect Fos in specific neuronal populations, additional sets of sections were reacted first for Fos (black nuclei), as explained above, followed by incubation in primary antisera containing one of the following antibodies: rabbit anti-orexin (1:5000), mouse anti-tryptophan hydroxylase (1:3000), rabbit anti-tyrosine hydroxylase (1:20,000), goat anti-choline acetyltransferase (1:1000), rabbit anti-corticotropin-releasing hormone (CRH; 1:2000), rabbit anti-arginine vasopressin (1:10,000), rabbit anti-Leu-enkephalin (1:2000), and rabbit anti-neurotensin (1:5000).

Characterization of primary antibodies. The rabbit polyclonal Fos antibody (Ab5; Oncogene Science) was generated using a synthetic peptide corresponding to the amino acids 4–17 of the human c-Fos protein as immunogen. The specificity of this antiserum was established in previous control studies in rat brain sections (Gaus et al., 2002). The immunogen used to generate the rabbit polyclonal orexin antibody (ab6214, lot #22008; Novus Biologicals) was a synthetic peptide that corresponds to the 14–33 aa of the bovine orexin A protein residue, conjugated to keyhole limpet hemocyanin with glutaraldehyde. The specificity of this antiserum has been demonstrated by the lack of labeling in brain sections from orexin knock-out mice. The tryptophan hydroxylase antibody (T0678, lot #092K4836; Sigma) is a mouse monoclonal (clone WH-3) antibody, and a recombinant rabbit tryptophan hydroxylase was used as immunogen. This antiserum reacts specifically with tryptophan hydroxylase (55 kDa) in immunoblotting assays (manufacturer's technical information) and stains a pattern of neuronal morphology and distribution identical to previous reports (Datiche et al., 1995). The rabbit polyclonal tyrosine hydroxylase (AB152, lot #22101229; Millipore Bioscience Research Reagents) was generated using SDS-denatured tyrosine hydroxylase from rat pheochromocytoma. By Western blot, this antiserum selectively labels a single band at ~62 kDa corresponding to tyrosine hydroxylase (manufacturer's technical information) and stains a pattern of neuronal morphology and distribution identical to previous reports (Takada, 1990). The affinity-purified goat polyclonal choline acetyltransferase antibody (AB144P, lot #0508007596; Millipore Bioscience Research Reagents) was generated by using the human placental enzyme as immunogen. It produces a 68–70 kDa band in immunoblotting assays (manufacturer's technical information) and stains a pattern of cellular morphology and distribution identical to previous reports (Armstrong et al., 1983). The rabbit polyclonal anti-CRH (T-4037, lot #970177-1; Peninsula) was generated using the synthetic peptide as immunogen. Radioimmunoassay shows cross-reaction only with human and rat CRH, not with related peptides (manufacturer's technical information). The rabbit polyclonal anti-neurotensin (NB 600–775, lot #170804) was generated using a synthetic peptide corresponding to the amino acid sequence QLYENLPRRPYIL. The specific immunostaining was abolished by preincubation with neurotensin (manufacturer's technical information). The rabbit monoclonal anti-arginine vasopressin (20069, lot #704156; Incstar) was generated using the peptide conjugated to bovine thyroglobulin with 1-ethyl-3-(3-dimethylaminopropyl) carbodiimide. The staining was completely eliminated by pretreatment of the diluted antibody with arginine vasopressin, but preadsorption with oxytocin had no effect on immunolabeling (manufacturer's technical information). The mouse monoclonal anti-dopamine β-hydroxylase (MAB308, lot #23090206; Millipore Bioscience Research Reagents) was generated using purified bovine dopamine β-hydroxylase as immunogen. This antibody labels neurons located in the classic noradrenergic groups extensively characterized in previous studies with other antibodies. The rabbit polyclonal anti-Leu-enkephalin was obtained from Dr. R. J. Miller (lot #1037, 1990). This antiserum was raised against synthetic Leu-enkephalin and stains a pattern of cellular morphology and distribution identical with previous reports (Hughes et al., 1977).

Fos analysis. For each experimental condition, we examined Fos immunoreactivity throughout the entire brain. For the ease of the reader in comparing the different conditions, we described Fos expression in the three main experimental groups (clean cage, cage exchange, and rats that were awake 50% of the time), using ranks assigned to each region depending on the level of Fos expression: 0 (none), 1 (scarce), 2 (low), 3 (moderate), and 4 (high). The rank average per area was calculated for each experimental group, and symbols were assigned as follows: 0 (0), from 0.1 to 1 (+), from 1.1 to 2 (++), from 2.1 to 3 (+++), and from 3.1 to 4 (++++). These symbols were used in Table 1. To simplify the comparison with the brains of rats with lesions or pharmacological manipulation, we described in the text the differences between those brains and the brains of cage exchange animals or clean cage controls. We also included a few photomicrographs from rats killed at 9:00 P.M., when they were spontaneously awake, to illustrate the main differences and similarities in the pattern of Fos expression with respect to the other groups, but we did not quantify the number of Fos-positive neurons in these rats.

In addition to these qualitative results, in all experimental groups Fos-immunoreactive neurons were quantified in brain regions involved in the sleep–wake circuitry, as well as in stress-sensitive areas that are part of cognitive and emotional pathways (limbic system). Fos-positive neurons were counted bilaterally at 10× in predetermined rectangular boxes of different size depending on the area of interest: for IFC, a 1040 × 1040 μm box placed medial to the forceps minor (bregma, 3.24 mm); for median preoptic nucleus (MnPO), a 624 × 728 μm box centered on the upper edge of the third ventricle (208 μm ventral, 520 μm dorsal; bregma, 0.12 mm); for ventrolateral preoptic nucleus (VLPO), a 728 × 624 μm box placed onto the ventral brain surface containing a smaller box for VLPO core (VLPOc; 312 × 312 μm) in the lower lateral corner, and the rest of the box was considered extended VLPO (VLPOex; bregma, −0.36 mm); for BST, a 416 × 832 μm box was placed ventral to the lateral ventricle and dorsal to the anterior commissure (bregma, −0.12 mm); CeA was centered in a 520 × 520 μm box (bregma, −2.76 mm). Fos in the TMN and the LC was counted at 25× with the help of a grid but without a counting box because of the clear location of the neuronal clusters along the brain surface in the case of the TMN (bregma, −3.96 mm) or along the fourth ventricle in the case of the LC (bregma, −9.84 mm). All bregma coordinates are from the rat brain atlas by Paxinos and Watson (1998). The average number of Fos-positive neurons in two to three sections (spaced 175 μm apart) was obtained for each area in all experimental groups. The numbers of Fos-positive neurons in the IFC shown in Figures 4 and 13 correspond to the total Fos counts in IFC divided by 2 because this brain region occupies a bigger area than the rest of regions quantified; therefore, the bars in these figures represent the number of Fos counts in a 520 × 1040 μm area. It was not necessary to use a correction factor for the Fos counts because the diameter of Fos-positive nuclei in each region did not differ among groups; thus the Fos counts represent relative numbers of profiles, not absolute numbers of cells.

To assess the neuronal activity of the parvicellular subdivisions of the PVH as an indicator of the ongoing stress response, we counted Fos-positive neurons in cage exchange and clean cage rats killed 90 min after being transferred or killed at 3:30 P.M. (four groups). Fos-positive neurons were counted bilaterally at 10× in a single section of the following: the anterior parvicellular PVH (apPVH) in a 624 × 624 μm box (bregma, −1.40 mm); the rostral part of the medial parvicellular PVH (rostral mpPVH) in a 1040 × 1040 μm box (bregma, −1.80 mm); and the caudal part of the medial parvicellular PVH (caudal mpPVH) in a 1040 × 1040 μm box (bregma, −2.12 mm). All boxes were centered over the PVH with the medial edge along the lateral wall of the third ventricle.

Statistical analysis. The percentages of wake, nREM, and REM sleep in controls and cage exchange rats from 7:00 A.M. to 3:30 P.M. were analyzed with repeated-measures ANOVA ($p < 0.05$), followed by a *post hoc* unpaired *t* test ($p < 0.05$) for each time point. The number of bouts for each state was analyzed from 11:00 A.M. to 3:30 P.M. using the same

tests. The number of bouts and mean duration of bouts for each state in the interval 2:00 to 3:30 P.M. (4 s epoch analysis) were analyzed using unpaired *t* tests ($p < 0.05$). The power spectrum ratio (ExpDay/BL × 100) was analyzed by comparing the average of all values (0.25 Hz intervals) for each frequency band using unpaired *t* tests ($p < 0.05$). The sleep latencies, the number of bouts, and the percentages of wake, nREM, and REM sleep in control, cage exchange, and treated rats (lesions or immepip injection) were analyzed with one-way ANOVA ($p < 0.05$), followed by Fisher's PLSD as a *post hoc* test ($p < 0.05$) for the first, second, fifth, and sixth hours. The percentages at each time point in control, cage exchange, and treated rats, shown in Figure 12, were analyzed with repeated-measures ANOVA followed by Fisher's PLSD ($p < 0.05$). The baseline sleep parameters (dark and light cycles) of controls were compared with the rest of groups (cage exchange, lesions, and immepip injections) using repeated-measures ANOVA ($p < 0.05$).

The numbers of Fos-positive neurons in control versus cage exchange rats were analyzed using unpaired *t* tests ($p < 0.05$) for each brain region. Comparisons among controls, cage exchange rats, and rats that were awake 50% of the time were done using one-way ANOVA followed by Fisher's PLSD as a *post hoc* test ($p < 0.05$). The same tests were used to compare controls, cage exchange rats, and treated rats (lesions or immepip treatment before cage exchange) and to compare Fos expression in the parvicellular subdivisions of the PVH in controls and cage exchange rats killed 90 min and 5.5 h after being transferred to a cage.

Results

Cage exchange as a model for stress-induced sleep disturbances

We chose cage exchange as a simple rodent model of sleep disturbances induced by a psychological stressor because we wanted to use a species-specific stimulus based on social context so we would not have to apply a continual, physical stressor. All rats had been habituated to changes into clean cages every few days at 10:00 A.M. for the previous 2–3 weeks. In the cage exchange paradigm, male rats were transferred at 10:00 A.M. (peak of sleep) either to a clean cage (controls) or to a dirty cage previously occupied by another male rat for 1 week (cage exchange). The odor of another rat is not a stressor per se because our rats are housed in adjacent cages and are continually exposed to each other's odors. What makes this stimulus a psychological stressor is the social setting of being inescapably surrounded by the territory that has been marked by another male rat. In their natural habitats, rats are very territorial, and exposure to the olfactory and visual cues of a competitor, even in the competitor's absence, induces a social and

Table 1. Fos expression in brain regions from the three experimental groups (regions included in Figure 4 are excluded here)

Area	Clean cage	Cage exchange	50% wake–sleep
Anterior olfactory nucleus	+	++++	+++
Orbital cortex	0	++++	+++
Prelimbic cortex	+	++++	++
Cingulate cortex	0	++++	++
Primary motor cortex	0	++++	++++
Secondary motor cortex	0	++++	+
Somatosensory cortex	0	++++	+++
Piriform cortex	+	++++	++++
Dorsal endopiriform nucleus	+	++++	+++
Agranular insular cortex	0	+	++++
Retrosplenial cortex	0	++++	++
Diagonal band	0	+	0
Lateral septum (dorsal)	0	+	++
Lateral septum (intermediate)	0	+++	++
Lateral septum (ventral)	+	++++	++++
Caudate putamen (dorsal)	0	++	0
Medial preoptic area	+	+	+
Lateral preoptic area	+	++	+
Anterodorsal preoptic area	++	+++	+++
Parastrial nucleus	+++	++++	++++
Suprachiasmatic nucleus	++++	++++	++++
Supraoptic nucleus	+	+	++++
Basal forebrain			
Medial septum	0	+	0
Diagonal band (horizontal limb)	0	0	0
Diagonal band (vertical limb)	0	0	0
Ventral pallidum	0	0	0
Magnocellular preoptic area	0	0	0
Substantia innominata	0	0	0
Magnocellular basal nucleus	0	0	0
Paraventricular hypothalamic nucleus			
Anterior parvicellular	0	+	++
Dorsal parvicellular	0	0	++
Ventromedial parvicellular	0	0	+++
Medial parvicellular (rostral)	0	++	++++
Medial parvicellular (caudal)	+	+++	++++
Magnocellular	0	0	+++
Retrochiasmatic area	+	++	++++
Subparaventricular zone	++++	++++	++++
Zona incerta	+++	++++	+++
Arcuate nucleus	+	+++	++++
Lateral hypothalamus/perifornical area	++	+++	+++
Dorsomedial hypothalamus (dorsal)	++	++++	+++
Dorsomedial hypothalamus (ventral)	+	++	++++
Dorsal hypothalamic area	+++	+++	++++
Ventromedial hypothalamus	0	0	0
Thalamus			
Paraventricular thalamic nucleus (anterior)	++	+++	+++
Central medial thalamic nucleus	+	++	+++
Anteroventral thalamic nucleus	0	++	+++
Rhomboid thalamic nucleus	+	++	+
Paraventricular thalamic nucleus (posterior)	++	+++	+++
Parafascicular thalamic nucleus	++	+++	++
Hippocampus			
Dentate gyrus	+	+++	+++
CA1–CA3 fields	0	++	+
Medial amygdala (dorsal + ventral)	0	+++	+
Premammillary nucleus (dorsal + ventral)	0	+++	+
Pretectal nucleus	++++	++++	++
Supramammillary nucleus	+++	++++	++
Intergeniculate leaf	++++	++++	+++
Superficial gray of superior colliculus	+	0	++++
Edinger-Westphal nucleus	++	++++	++
Ventral tegmental area (nondopaminergic)	0	++	0
Ventral tegmental area (dopaminergic)	0	+	0

(*Table continues.*)

Table 1. Continued

Area	Clean cage	Cage exchange	50% wake–sleep
Rostral linear nucleus of the raphe (dopaminergic)	+	++++	+
Caudal linear nucleus of the raphe (dopaminergic)	0	++++	0
Interfascicular + interpeduncular nuclei	0	++	0
Dorsal raphe (serotoninergic)	0	+	0
Dorsal raphe (nonserotoninergic)	0	++	++
Periaqueductal gray			
Lateral	+	++	+++
Dorsal	++++	++	+++
Ventral (dopaminergic)	0	+	0
Ventral (nondopaminergic)	+	++	+++
Ventrolateral	++	+++	+
Pedunculopontine tegmental nucleus (noncholinergic)	++	++++	++
Laterodorsal tegmental nucleus (noncholinergic)	++	++++	++
Lateral parabrachial nucleus	++	+++	++
Dorsal tegmental nucleus	0	0	++++
Reticulotegmental nucleus	+++	++++	+++
A7 group	+	++	++
A5 group	+	+++	++
Barrington's nucleus	+	+++	++
Nucleus O	+	++++	+
Caudal raphe (raphe pallidus + raphe magnus)	++	++	+++
Subcoeruleus nucleus (dorsal + ventral)	++	++	+++
Pontine reticular nucleus (caudal)	0	+	+++
Gigantocellular reticular + intermediate reticular nuclei	0	+	++++
Lateral paragigantocellular nuclei	+++	++	+++
Dorsal paragigantocellular nucleus	0	+	+++
Parvicellular reticular nucleus	++	+++	++++
Medial vestibular nucleus	++++	++	+++
Cuneate + external cuneate nuclei	++	+++	+++
Rostroventrolateral medulla	+++	+++	+++
C3 group	++++	+++	+++
Nucleus of the solitary tract (medial)	+	++	+
Nucleus of the solitary tract (ventrolateral)	0	+	+++
Dorsal motor nucleus of the vagus	0	0	++
Area postrema	++	++	+
Caudoventrolateral medulla	+++	+++	++
Medullary reticular nucleus (dorsal)	+++	0	++++
Medullary reticular nucleus (ventral)	0	0	++

The pattern of Fos in rats that are spontaneously awake 50% of the time differs from that observed in cage exchange rats. In general, the cortex showed less Fos than in cage exchange rats, with the exception of the agranular insular and primary motor cortices. Conversely, all divisions of the PVH (parvicellular and magnocellular) and the supraoptic nucleus showed higher levels of Fos than in cage exchange rats, which may be due to circadian influences because this group of rats was killed at 6:50 P.M., right before the onset of the active period at 7:00 P.M. The retrochiasmatic area, arcuate nucleus, and the ventral part of the dorsomedial hypothalamus also showed more Fos in rats awake 50% of the time. The pattern of Fos in the periaqueductal gray differs between the two groups; cage exchange rats show more Fos in the ventrolateral division, whereas rats awake 50% of the time had more Fos in the dorsal and lateral divisions. The superficial gray matter of the superior colliculus and the dorsal tegmental nucleus were highly activated exclusively in rats awake 50% of the time but neither in cage exchange nor in controls. In general, the brainstem was slightly more active in rats that were awake 50% of the time than in cage exchange rats. Ranks were scored as follows: 0 (none), + (scarce), ++ (low), +++ (moderate), and ++++ (high) levels of Fos expression.

psychological species-specific stress response (Oka et al., 2001). Although this model is not entirely analogous to all subtypes of stress-induced insomnia in humans, which usually occurs under heterogeneous conditions, it is sufficiently similar as to be a reasonable starting point for analyzing how stress affects sleep circuitry in the brain.

The initial handling and the novelty of being transferred to a new cage caused an increase in body temperature of 0.95 ± 0.14°C in the clean cage controls and of 1.29 ± 0.09°C in the cage exchange rats (Fig. 1*A*). This initial stress response was accompanied by increased expression of Fos protein, a transcription factor widely used as a marker of neuronal activity, in the mpPVH, which contains neurons that secrete CRH into the median eminence and initiate the classical adrenocortical stress response. The majority of stressors induce Fos expression in the rostral part of the mpPVH at the level of the magnocellular subdivision that contains vasopressin neurons (bregma, −1.80 mm); however, in the cage exchange paradigm, Fos expression was increased mainly in the caudal part of the mpPVH (bregma, −2.12 mm), which contains CRH-secreting neurons and also neurons involved in autonomic control. Thus, in rats killed 90 min after cage change, Fos expression in the caudal mpPVH was higher in cage exchange rats than in clean cage controls (352.3 ± 9.2 vs 222.5 ± 8.5; $p = 0.0319$) (Fig. 1*B–D*), whereas in the rostral mpPVH, Fos expression was similar in both groups (130.5 ± 29.5 for controls vs 175.3 ± 30.14 for cage exchange rats; $p = 0.5911$) (Fig. 1*B*) and lower than in the caudal part. In addition, there was some Fos expression in the ap-PVH in both groups (66.0 ± 3.0 in controls, 71.33 ± 7.6 in cage exchange rats). However, 5–6 h after cage exchange, these initial indices of an acute stress response had disappeared in the clean cage controls and diminished in the cage exchange rats. Temperature returned to normal levels in both groups; although it appeared slightly elevated in cage exchange rats (0.2°C higher than controls), this difference was not statistically significant (Fig. 1*A*). Fos expression in the mpPVH (rostral and caudal) was minimal in clean cage controls (Figs. 1*B*,*E*) and was substantially decreased in cage exchange rats compared with rats killed 90 min after cage exchange (193.9 ± 22.2 at 5.5 h vs 352.3 ± 9.2 at 90 min in the caudal mpPVH; $p = 0.007$) (Fig. 1*B*). Nevertheless, Fos in the mpPVH was highly variable in cage exchange rats (killed 5.5 h after exposure) (Fig. 1*H*), consistent with previous studies reporting marked interindividual differences in stress responses among rats (i.e., low and high responders) (Sarkisova and Kolomeitseva, 1993; Bouyer et al., 1998). However, cage exchange rats remained hyperaroused 5–6 h after initial stress, with diminished and fragmented sleep, and with a specific pattern of Fos activity. This model permitted us to study the long-term effects of psychological stress on the brain circuitry involved in sleep regulation because the animals had adapted to the initial stress and their sleep disturbances were maintained by the ongoing cognitive response to a social situation.

After being placed in new cages (clean or dirty), all rats in both groups were awake for most of the next hour, although control rats had a shorter latency to fall asleep than cage exchange rats (31.8 ± 3.4 vs 58.7 ± 7.4 min; $p = 0.0086$). After this first hour, control rats slept normally for the rest of the light period. In contrast, cage exchange rats showed increased wakefulness during the second hour after cage exchange (45.9 ± 5.9% compared with 22.5 ± 3.6% in clean cage controls; $p = 0.011$) (Fig. 2*A*), as well as decreased nREM (47.7 ± 5.2% vs 62.3 ± 4.9%; $p = 0.079$) (Fig. 2*C*) and REM (6.4 ± 1.4% vs 15.2 ± 2.2%; $p = 0.0019$) sleep (Fig. 2*E*). During the third and fourth hours after cage exchange, rats transferred to dirty cages had normal amounts of nREM

sleep and wake, presumably because of the circadian drive and the increased homeostatic pressure caused by the sleep loss in the first 2 h. Nevertheless, in this period REM sleep was decreased and there was an increased number of wake bouts (increased fragmentation; from 12.9 ± 1.1 bouts in controls to 17.3 ± 0.8 in cage exchange rats during the third and fourth hours after cage exchange; $p = 0.0054$) (Fig. 2*B*). During the fifth and sixth hours after cage exchange, the rats in dirty cages showed increased wakefulness (46 ± 3.4% vs 22.9 ± 2.1% in controls; $p = 0.0076$) (Fig. 2*A*), and decreased nREM (43.4 ± 3.3% vs 58.2 ± 2.0%; $p = 0.0378$) (Fig. 2*C*) and REM sleep (10.7 ± 5.9% vs 18.8 ± 2.2%; $p = 0.0423$) (Fig. 2*E*). The experimental model and the temporal sequence of sleep disturbances are summarized in Figure 3. It is important to point out that cage exchange rats were not fully awake during this late insomnia period; they slept 25% less than controls, but they did sleep, similar to what happens in transient insomnia induced by stress and anxiety in humans (Bonnet and Webb, 1976; Toussaint et al., 1997).

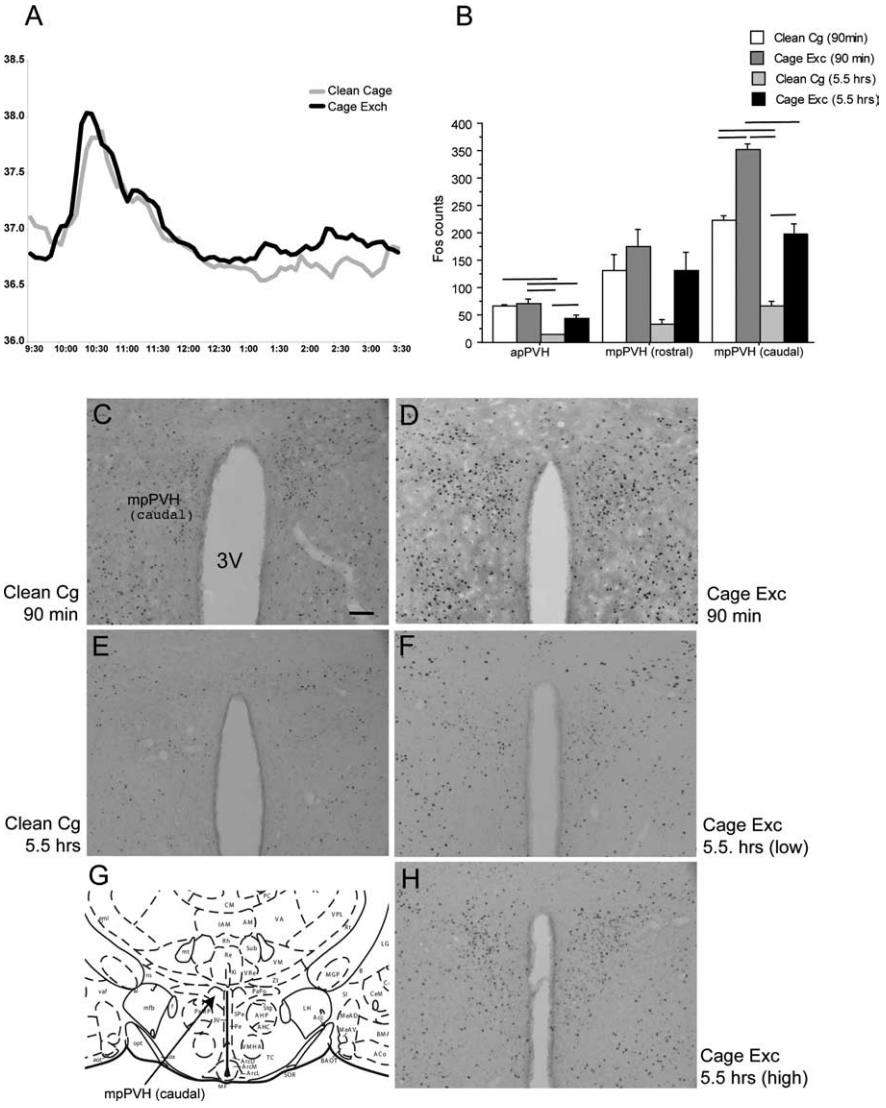

Figure 1. ***A***, Stress-induced hyperthermia peaks at 10:30 A.M. in rats transferred to a clean cage (0.95 ± 0.14°C) or a dirty cage (1.29 ± 0.09°C) at 10:00 A.M. and returns to basal levels after 1 h. During the sleep disturbance period, temperature is slightly higher in cage exchange (Cage Exch) rats (0.2°C), but not significantly different from controls. For the sake of clarity, error bars have been omitted in this graph that plots temperature every 5 min, but none of the time points is statistically different between the two groups. ***B–H***, Fos counts in several parvicellular subdivisions of the PVH are higher in rats killed 90 min after cage exchange (Cage Exc; ***D***) than in rats killed 5.5 h after cage exchange (***F***, ***H***) and rats killed 90 min after being transferred to a clean cage (Clean Cg; ***C***), which have similar numbers of Fos counts. Clean cage controls killed after 5.5 h (***E***) showed little Fos immunoreactivity. Photomicrographs show Fos expression in all these experimental groups at the level of the caudal mpPVH (bregma, −2.12 mm) as shown in the template (***G***) modified from Figure 26 of the rat brain atlas by Paxinos and Watson (1998) with permission from Elsevier. Rats killed 5.5 h after cage exchange showed high variability in Fos expression, ranging from rats with little Fos expression (***F***) to animals with extensive Fos (***H***). In ***B***, data for each parvicellular subdivision were analyzed with one-way ANOVA followed by Fisher's PLSD (horizontal bars at top indicate significant differences, $p < 0.05$). All values are the mean ± SEM. Scale bar, 100 μm. 3V, Third ventricle.

Fos expression discloses coactivation of sleep and arousal systems during stress-induced sleep disturbances

To study the brain areas activated during stress-induced insomnia, we killed the rats 90 min after the onset of the late period of insomnia (5.5 h after cage exchange) and processed the brains for the presence of Fos. In general, the brains of cage exchange rats showed more extensive Fos expression than controls, which had Fos levels similar to sleeping animals in previous studies from our laboratory setting (Estabrooke et al., 2001; Ko et al., 2003). In cage exchange rats, Fos expression was elevated in several components of the arousal system, specifically the TMN and the LC (Figs. 4, 5). Other components of the arousal system that are usually active during wakefulness, such as the noncholinergic neurons in the basal forebrain, the dopaminergic neurons in the ventral periaqueductal gray matter, and the orexin neurons in the lateral hypothalamus (LH), did not show Fos immunoreactivity (Table 1). However, there was Fos expression in the majority of orexin neurons in the group of rats killed 90 min after cage exchange (Fig. 6), when the animals had been mainly awake, in agreement with previous studies reporting that orexin neurons are activated by stress (Ida et al., 2000; Kuru et al., 2000; Sakamoto et al., 2004; Winsky-Sommerer et al., 2004) and during wakefulness (Chemelli et al., 1999; Lee et al., 2005; Mileykovskiy et al., 2005). Other arousal neuronal groups, such as the serotoninergic raphe neurons, and the cholinergic neurons in the basal forebrain and in the laterodorsal tegmental nucleus (LDT) and pedunculopontine tegmental nucleus (PPT), generally do not show Fos expression during wakefulness, and also did not express Fos during this sleep disturbance period (Table 1).

Fos expression was also increased in the limbic system in cage exchange rats (Figs. 4, 7). Although there was a generalized increase in Fos expression throughout the cerebral cortex, it was especially intense in the IFC, which has an important role in attention, reward, and modulation of stress responses (Sullivan and Gratton, 2002; Dalley et al., 2004), as well as in the cingulate cortex; in the lateral septum and the hippocampus; and in the CeA and the lateral division (dorsal and posterior subnuclei) of

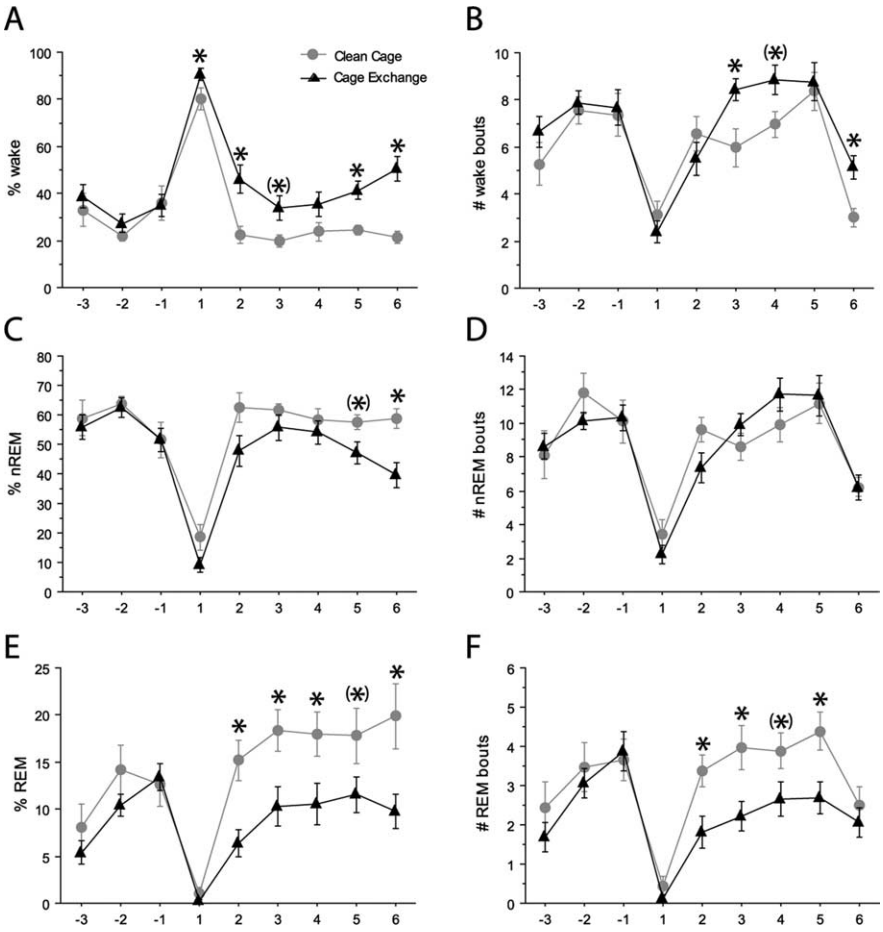

Figure 2. Species-specific stress causes initial and late sleep disturbances (acute insomnia). ***A***, ***C***, Rats that are placed in a cage previously occupied by another male rat (cage exchange) sleep significantly less during the first and second hours (initial stress response) and during the fifth and sixth hours (stress-induced acute insomnia) after cage exchange. ***E***, There is loss of REM sleep across the entire period. ***B***, ***D***, ***F***, The number of nREM bouts is not different (***D***) between controls and stressed rats, but there are fewer transitions from nREM to REM sleep (***F***), and more to wakefulness (***B***), indicating a period of sleep fragmentation. The *x*-axis is marked in hours before or after the cage exchange. Data were analyzed by repeated-measures ANOVA, followed by unpaired *t* tests for comparisons at each time point. $^{*}p < 0.05$; $^{(*)}p$ between 0.05 and 0.09. All values are the mean ± SEM.

the BST, two areas involved in fear, anxiety, and emotional processing (Davis and Shi, 1999; Phelps and LeDoux, 2005). The pattern of Fos expression in the parvicellular subdivisions of the PVH has been described in the previous section (see Table 1). Regions involved in central autonomic control also had increased Fos during the sleep-disturbed period, including nonorexin neurons in the LH, the dorsomedial hypothalamic nucleus (DMH), the ventrolateral periaqueductal gray matter (vlPAG), the lateral parabrachial nucleus, the A7 and A5 noradrenergic groups, and the ventrolateral medulla (Table 1). Elevation of sympathetic activity is typically observed during stress-induced insomnia in humans (Vgontzas et al., 1998; Richardson and Roth, 2001), although we did not measure it in our rats.

Unexpectedly, despite the poor quality of sleep (lower percentage of time spent sleeping and increased fragmentation) during this period, we found extensive Fos expression in each of the forebrain sleep-promoting areas, including the VLPOc, VLPOex, and MnPO. Each of these groups showed at least as many Fos-positive neurons as sleeping controls or even more in the case of the VLPOex (Figs. 4, 5).

The simultaneous activation of the sleep and arousal systems observed in cage exchange rats during the period of sleep disturbances is surprising because it is believed that the two systems reciprocally inhibit each other under normal conditions (sleep or wake), and therefore when one system is fully active the other should be inhibited (McGinty and Szymusiak, 2000; Saper et al., 2001). However, the time resolution of Fos protein expression is on the order of 1–2 h; therefore, our results could reflect alternate rather than simultaneous activation of the wake and sleep systems during this late sleep disturbance period because these cage exchange rats slept ~50% of the time. To determine whether this was the case, we examined the pattern of Fos expression in the brains of rats killed at 6:50 P.M. (a time of the day when they had naturally slept undisturbed 50% of the previous 90 min). Fos counts in the three sleep-promoting areas in these rats were ~40% lower than those in cage exchange rats, even though both groups had slept ~50% of the previous 90 min (98.7 ± 5.1 Fos-positive cells in the naturally sleeping rats vs 161.6 ± 11.9 in the MnPO in cage exchange rats; $p = 0.0356$; 34.1 ± 2.7 vs 53.3 ± 2.3 in the VLPOc; $p = 0.0008$; and 73.3 ± 5.1 vs 126.9 ± 8.3 in the VLPOex; $p = 0.0036$); indeed, the Fos expression in these brain areas in cage exchange rats was similar to clean cage control rats that slept 75–80% of the time (Figs. 4, 5). These results demonstrate that the high level of Fos expression in the sleep-promoting system during the period of sleep disturbances induced by stress is not simply a reflection of the fact that the rats spent 50% of their time asleep.

In contrast, the levels of Fos expression in the cortex of rats that spontaneously slept 50% of the time were intermediate between the clean cage controls (almost no Fos) and the cage exchange rats [which had Fos levels similar to those of rats killed at 9:00 P.M. that had been spontaneously awake (Fig. 5)]. With respect to the limbic system, Fos expression in the IFC and CeA of rats that slept 50% of the time was much less than in cage exchange rats (153.2 ± 13.1 vs 305.1 ± 22.2 for IFC; $p = 0.0027$; 73.7 ± 3.6 vs 147.1 ± 11.9 for CeA; $p = 0.0064$) and similar to clean cage controls (118.4 ± 25.6 for IFC; 75.1 ± 9.7 for CeA), whereas the level of Fos in the BST (91.1 ± 5.2) was intermediate between controls (60.1 ± 7.9) and stressed rats (124.1 ± 9.9) (Fig. 4). These results suggest that activation of the limbic system is a specific component of the circuitry involved in the stress-induced sleep perturbation and not caused by the fact that the rats were awake 50% of the time. With respect to the arousal system, the LC did not show Fos in animals that had been spontaneously awake 50% of the time, but the Fos expression in the TMN was similar to cage exchange rats (Figs. 4, 5). Thus, Fos expression in the LC seems to be specific for stress-induced insomnia (and in fact was even higher than in waking controls at 9:00 P.M.), whereas Fos in the TMN seems to reflect the degree of wakefulness in any condition. In general, Fos expression in rats that had spontaneously been awake 50% of the time was intermediate between waking

rats and sleeping controls, and quite different from cage exchange rats, which also slept 50% of the time (Table 1).

It is important to mention that some of the differences in Fos expression between rats that had spontaneously been awake 50% of the time and cage exchange rats or controls could be caused by circadian influences because these groups were killed at different zeitgeber times (6:50 P.M. is ZT 11:50, and 3:30 P.M. is ZT 8:30, respectively). Indeed, some brain regions such as the PVH (parvicellular and magnocellular subdivisions) and the supraoptic nucleus have higher Fos expression in rats that have been awake 50% of the time than in cage exchange rats, which may reflect the normal activation of these brain areas preceding the onset of the active period at 7:00 P.M.

In summary, the pattern of Fos activation observed during the late period of sleep disturbances induced by stress suggests that this period is a distinct behavioral state, which differs from both sleep and wakefulness (Fig. 5). There is Fos expression in the LC, which usually has few if any Fos-immunoreactive neurons during undisturbed wakefulness or sleep, and in the sleep-promoting areas, which normally show similar levels of Fos activity only after persistent sleep. Moreover, the Fos pattern was different from that initially elicited by acute stress, because Fos activity was substantially decreased in the pvPVH and eliminated in orexin neurons at 5.5 h after cage exchange. Therefore, the unique pattern of Fos expression during stress-induced sleep disturbances in rats appears to reflect the ongoing cognitive and emotional responses caused by psychological stress, which outlast the initial acute stress response.

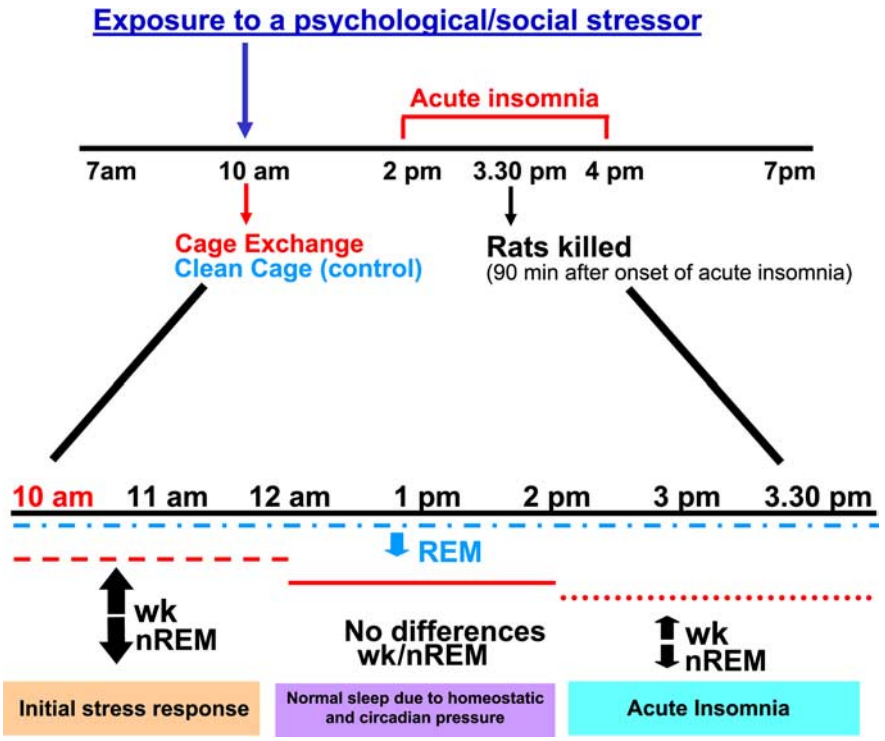

Figure 3. Rats typically sleep mainly during the light cycle, from 7:00 A.M. to 7:00 P.M. At 10:00 A.M. (peak of sleep), we place a male rat in a dirty cage that has been previously occupied by another male rat for 1 week, which induces a generalized stress response (fight or flight). Control rats are placed in clean cages. Stressed rats are mostly awake during the first 2 h after cage exchange compared with controls. The next 2 h, stressed rats sleep more or less normally as a result of the homeostatic and circadian drives. This is followed by a 2 h period of sleep disturbances in stressed rats in which they sleep ~20% less than controls. REM sleep is decreased along the whole period after cage exchange. This period of stress-induced acute insomnia 4–6 h after cage exchange (from 2:00 to 4:00 P.M.) is consistently observed in all rats. To assess what brain areas are activated, rats were killed at 3:30 P.M., 90 min after the beginning of this late period of sleep disturbances (optimal time for detection of Fos evoked by a specific stimulus). wk, Wake.

Physiological evidence for simultaneous activation of sleep and arousal circuitry during stress-induced sleep disturbances

We hypothesized that the unique pattern of simultaneous Fos expression in both sleep and arousal systems in our cage exchange rats might be caused by frequent and brief transitions between states (microbouts). We therefore reanalyzed the sleep recordings during the late period of sleep disturbances (2:00 to 3:30 P.M.) using 4 s epochs to determine whether we missed such fast transitions when data were originally analyzed using 12 s epochs. We found that the number of wake and nREM microbouts was not significantly increased in cage exchange rats with respect to controls, although the number of REM microbouts was decreased (10.2 ± 1.4 vs 5.4 ± 0.6 bouts; $p = 0.0013$) (Fig. 8*A*), as was overall REM sleep in the cage exchange animals. These results suggest that the pattern of Fos observed in cage exchange rats is not caused by frequent and brief transitions between sleep and wakefulness. Nevertheless, cage exchange rats showed a trend to have longer wake bouts (32.1 ± 6.0 vs 60.6 ± 9.7 s; $p = 0.051$) and shorter nREM bouts (138.0 ± 12.0 vs 114.0 ± 7.6 s; $p = 0.088$) during this period (Fig. 8*B*), which accounts for the difference in percentage of wake and nREM sleep with respect to controls.

The other possibility to explain the observed pattern of Fos expression is that indeed both sleep and arousal systems are activated at the same time. We analyzed the EEG power spectrum (4 s epochs) during the late period of sleep disturbances and found that cage exchange rats have increased high-frequency EEG activity in the gamma band (30.5–58 Hz; $p < 0.0001$) during nREM sleep (Fig. 8*C*,*D*), but, in contrast, had no differences in delta power with respect to controls. High-frequency EEG activity, which is characteristic of wakefulness, is associated with cortical activation, and cage exchange rats also showed high levels of Fos in the cortex, similar to spontaneously awake rats, even though they were sleeping 50% of the time. This cortical activation during nREM sleep may be caused by the LC and TMN, because these nuclei provide dense innervation to the cortex and are Fos positive during this stress-induced insomnia period. These results suggest that both sleep-promoting areas and part of the arousal system are most likely simultaneously activated during the period of stress-induced sleep disturbances.

It is important to mention that in our rats, the high-frequency activity during nREM sleep occurs in the gamma range, whereas in humans with insomnia, similar high-frequency activity is mainly observed in the beta range and to a lesser extent in the gamma range (Perlis et al., 2001a). However, Maloney et al. (1997) have reported that in rats, gamma activity, not beta, reflects behavioral and cortical arousal associated with attentive-

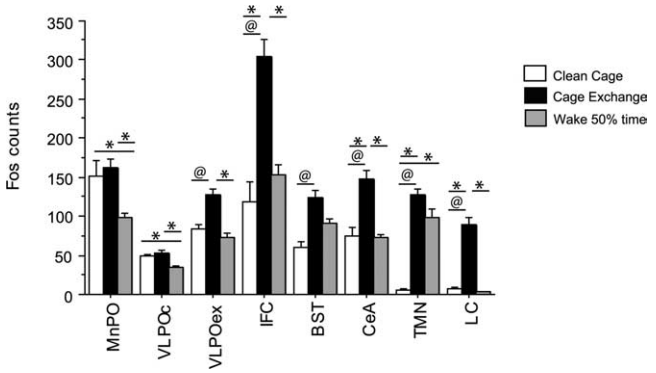

Figure 4. Previous exposure to a stressor (cage exchange 5–6 h before) induces Fos expression in neurons in both sleep-promoting areas (MnPO, VLPOc, and VLPOex) and arousal systems, including the limbic system (IFC, BST, and CeA) and wake-promoting areas (TMN and LC). Fos expression was substantially lower in the clean cage controls (which were sleeping normally at this time) in all regions except in the sleep-promoting areas, MnPO and VLPOc, in which it was comparable to stressed animals. Rats with amounts of spontaneously occurring sleep (awake 50% of the time during the previous 90 min) similar to the amounts of sleep in stressed rats in hours 5 and 6 had lower Fos counts than stressed animals in all regions except in the TMN, where Fos counts are thought to mirror recent waking behavior. In a first analysis, we compared controls and stressed rats, using an unpaired *t* test for each area, to determine whether there were differences in Fos expression as a result of the treatment (@for comparisons between these two groups, $p < 0.05$). In a second analysis, we compared the three groups (controls, stressed rats, and rats spontaneously awake 50% of the time), using a one-way ANOVA followed by Fisher's PLSD, to determine whether the differences we observed in the first analysis were attributable to the fact that stressed rats were awake 50% of the time (*for pair comparisons among the three groups, $p < 0.05$). All values are the mean ± SEM.

ness, sensory perception, and focused arousal. Therefore, the gamma activity during nREM sleep found in cage exchange rats might be analogous to the beta/gamma activity observed in humans experiencing insomnia.

Inactivation of selected brain regions has differential effects on sleep and Fos expression during stress-induced sleep disturbances

To study the role of selected brain areas that showed elevated Fos expression during stress-induced insomnia, we inactivated specific components of the limbic system (IFC and CeA–BST), using ibotenic acid lesions, or the arousal system, using 6-OH-dopamine lesions (to inactivate the LC) or intraperitoneal injections of immepip, and then analyzed the patterns of sleep and Fos expression. Immepip is an H3 receptor agonist that inhibits histaminergic neurons by binding to somatodendritic H3 autoreceptors in the TMN (Jansen et al., 1998), and that may also bind to presynaptic H3 receptors on TMN and possibly LC axon terminals (Schlicker et al., 1994; Brown et al., 2001).

Injections of cell-specific toxins almost never completely destroy the target site and almost always have some overlap into adjacent areas. Our lesions were reasonably selective and specific to the structure aimed, although in some cases they extended into part of adjacent regions. Two rats with CeA/BST lesions were removed from the study because the lesion aimed at the CeA was small and out of the target. The placement of representative lesions is shown in the photomicrographs of Nissl-stained sections (Fig. 9), whereas the extent of all bilateral lesions is shown in supplemental Figures 1 and 2, *A* and *B* (available at www.jneurosci.org as supplemental material). The average percentage of remaining neurons after lesions with respect to controls, assessed in Nissl-stained sections, was 0.2 ± 0.05% for the IFC, 13.6 ± 1.7% for the BST, and 10.3 ± 2.2% for the CeA. There were 21.2 ± 5.7 remaining noradrenergic neurons per set of sections labeled for dopamine β-hydroxylase in rats with LC lesions. We were unable to count the total number of LC neurons in control rats because they are tightly clustered in the relatively thick sections that we used, but based on an estimated of 3285 neurons in the LC of the adult albino rat from a previous study (Swanson, 1976), this number represents ~2.6 ± 0.7% of the neurons remaining after LC lesions. The lesions with 6-OH-dopamine were specific to the LC, because other noradrenergic groups in the brainstem were intact.

To analyze whether there were interindividual variations in the physiological responses in relation to the extent of the lesion was difficult because the range of percentage of remaining neurons after lesions in the IFC or the LC was very narrow (from 0.05 to 0.31% and from 1.3 to 5.3%, respectively). In the case of the CeA/BST lesions, the ranges were larger (11.1–20.1% remaining neurons in BST lesions and 5.9–18.1% in CeA lesions), but the combination of two lesions with different extent in the same animal complicates this kind of analysis. Nevertheless, we performed a regression analysis for the percentage of remaining neurons versus percentage of state (wake, nREM, and REM) in the sleep-disturbed period (2:00 to 3:30 P.M.) for CeA lesions and BST lesions independently (supplemental Fig. 3, available at www.jneurosci.org as supplemental material). We found that in all cases, the points were clustered and the R^2 values were very low, suggesting that the small differences in the extent of the lesions were not enough to produce a profound variation in the physiological responses.

We chose these structures from the many that showed Fos activation (Table 1) based on their hypothesized role in arousal and stress, and their known anatomical interconnections. Although other brain structures undoubtedly are involved in this circuitry, the importance of the areas we selected was demonstrated by our observations that inactivating them had distinctive effects on different aspects of the disturbed sleep. The results of these studies are organized according to the sleep component analyzed, instead of by lesions, and in chronological order as follows.

Sleep baseline

There were no differences between lesioned (IFC, CeA–BST, or LC) and nonlesioned (control and cage exchange) rats in the total amount of baseline nREM, REM, and wake, during the dark and light phases (supplemental Figs. 4, 5, available at www.jneurosci.org as supplemental material). Our data agreed with previous reports that LC lesions did not change sleep in baseline conditions (Lu et al., 2006; Blanco-Centurion et al., 2007). The average number of nREM, REM, and wake bouts per hour was not significantly different in the dark period. The only significant difference we found was that the average number of REM bouts per hour in the light period was higher in rats with CeA–BST lesions than in control and cage exchange rats (one-way ANOVA, $p = 0.0021$; followed by Fisher's PLSD for pair comparisons, $p = 0.0058$ for controls and $p = 0.002$ for cage exchange rats), although this difference was not very pronounced (4.83 ± 0.42 REM bouts per hour for CeA–BST-lesioned rats vs 3.67 ± 0.22 and 3.40 ± 0.16 for controls and cage exchange rats, respectively). The distribution of percentage of each state (nREM, REM, and wake) by hour along the dark and light periods was analyzed in rats with IFC lesions or CeA–BST lesions and compared with controls and cage exchange rats using a repeated-measures ANOVA ($p < 0.05$); we did not find any significant difference between the lesioned groups and the other two groups (p be-

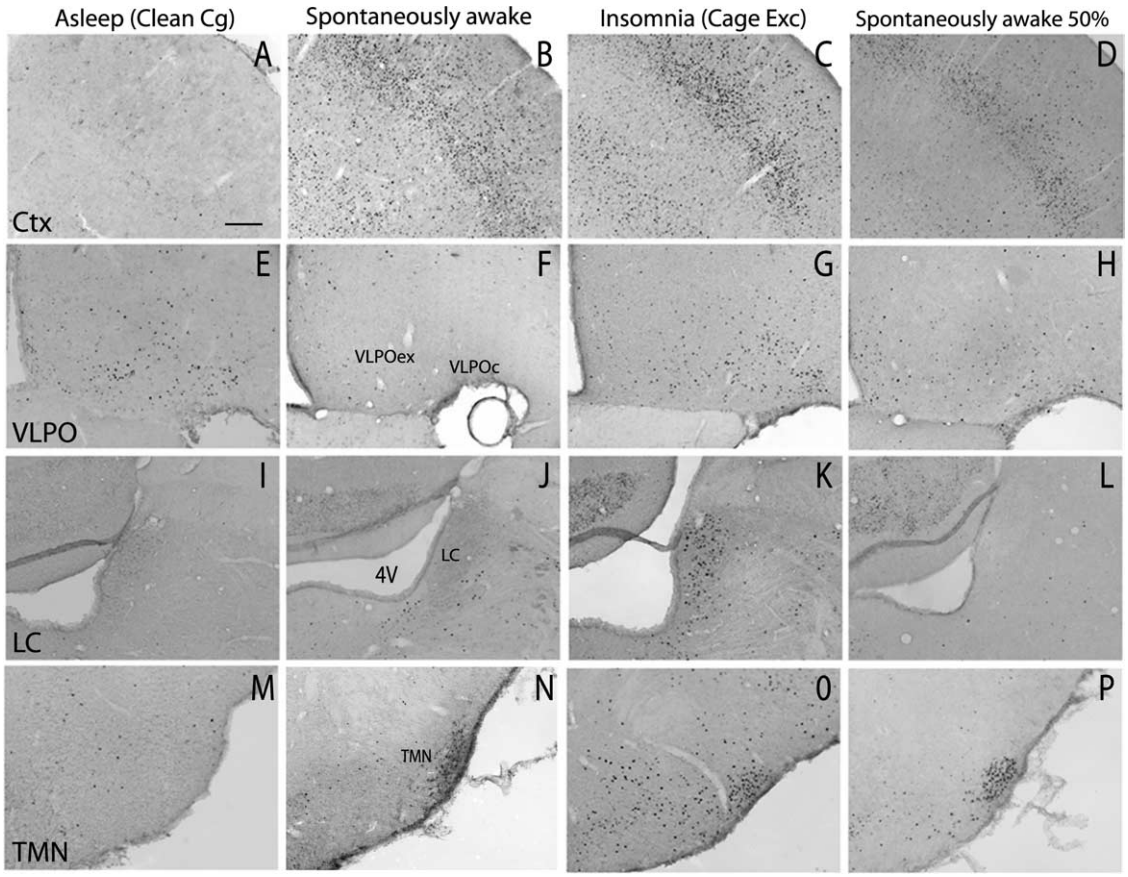

Figure 5. Fos activation in the brain during stress-induced insomnia differs from both wake and sleep states. The somatosensory cortex (Ctx; ***A–D***), VLPO (***E–H***), LC (***I–L***), and TMN (***M–P***) are shown in all three states, as well as in rats that have spontaneously naturally slept 50% of the previous 90 min period. Note that cage exchange (Cage Exc) rats show activation of the cortex and TMN that is equivalent to wakefulness, and even higher activation of the LC, but paradoxical simultaneous activation of the VLPO, similar to that observed in sleeping rats. Scale bar, 200 μm. 4V, Fourth ventricle; Cg, cage.

tween 0.2270 and 0.5728) (supplemental Fig. 2, available at www.jneurosci.org as supplemental material). These results suggest that in general the lesioned areas are not essential for maintaining the normal amount of sleep–wakefulness, although the observations below indicate that they are recruited by the stress response to generate the sleep perturbations observed after cage exchange. Although the amount of REM sleep was not altered, the CeA and BST seem to play a role in the regulation of the number of REM bouts in the light period, which is in agreement with the well established notion that emotions (i.e., the limbic system) can modulate REM sleep.

Sleep latency

Unlesioned cage exchange rats took almost twice as long to fall asleep compared with controls in clean cages (58.7 ± 7.5 vs 31.7 ± 3.4 min; $p = 0.0037$) (Fig. 10*A*). The sleep latency in rats with IFC lesions after cage exchange (63.6 ± 8.6 min) did not differ from unlesioned cage exchange rats, whereas CeA–BST lesions decreased sleep latency to the levels of controls (40.5 ± 4.7 min; $p = 0.3850$). Rats with LC lesions or immepip treatment before cage exchange showed a 10 min decrease in sleep latency with respect to unlesioned cage exchange rats (48.5 ± 8.4 and 48 ± 1.6 min, respectively), but this difference was not statistically significant. These results suggest that the activation of the CeA–BST is required to cause the difficulty in falling asleep after cage exchange, but there may also be participation of the LC and TMN, which receive projections from the CeA–BST.

Sleep during the first 2 h after cage exchange

The first hour after cage exchange corresponds to the initial stress response, and as expected, all groups transferred to dirty cages had increased wakefulness (Fig. 10*B*) and decreased nREM sleep (Fig. 10*C*) compared with controls in clean cages. REM levels were minimal in all groups, including controls, during this first hour (Fig. 10*D*). During the second hour, clean cage controls showed normal sleep for that time of the day, and only the cage exchange rats with CeA–BST lesions fell asleep similarly, whereas the other groups had increased wake and decreased nREM compared with controls (Fig. 10*B*,*C*). Rats with LC lesions had a trend toward recovery of nREM (not statistically significant) in this period, but REM was decreased in all groups during this second hour (Fig. 10*D*). These results suggest that all experimental groups were responsive to the initial stress associated with cage exchange, because all showed sleep disturbances during the first hour after exposure. Difficulties with falling asleep during the second hour seem to be mainly mediated by the CeA–BST, but may to a lesser extent be influenced by the LC.

Sleep fragmentation during the third and fourth hours after cage exchange

The number of wake bouts and nREM bouts during the period when cage exchange rats showed sleep fragmentation (third and fourth hours after cage exchange) was decreased to control levels after IFC lesions, LC lesions, and immepip treatment, whereas CeA–BST lesions had no effect (Fig. 11). The number of REM

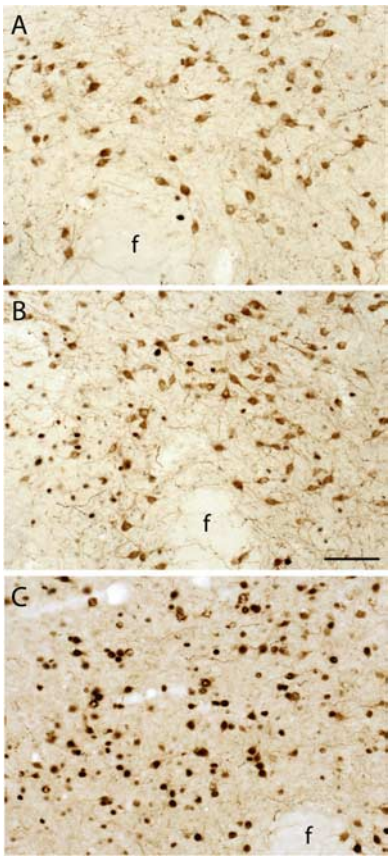

Figure 6. ***A–C***, Fos activation (black nuclei) in orexin neurons (brown staining) in the lateral hypothalamus–perifornical area during sleep (***A***), stress-induced acute insomnia (***B***), and initially after cage exchange (mainly wakefulness) (***C***). Note that the orexin neurons are normally active during wakefulness but not during normal or disturbed sleep. Scale bar, 200 μm. f, Fornix.

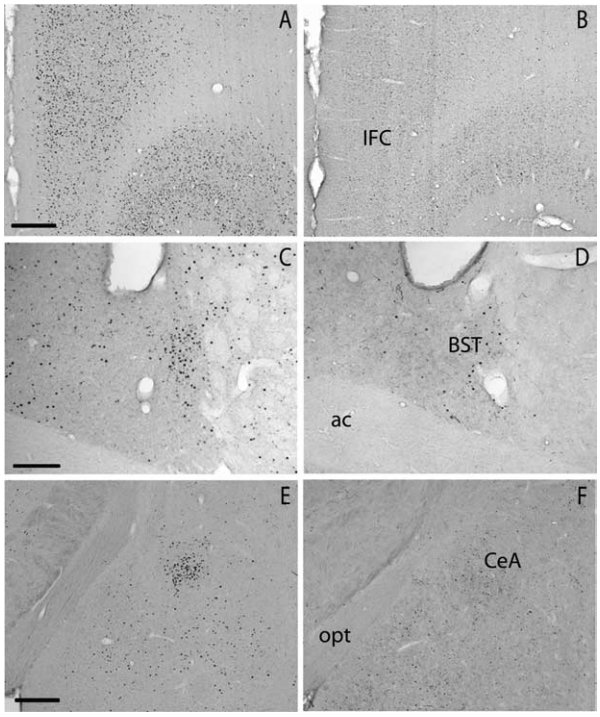

Figure 7. The high levels of Fos expression in the IFC, BST, and CeA demonstrate that portions of the limbic system are strongly activated during stress-induced insomnia (4–6 h after cage exchange; ***A***, ***C***, ***E***) but not during normal sleep (clean cage controls at the same time; ***B***, ***D***, ***F***). Scale bars: ***A*** (for ***A***, ***B***), ***E*** (for ***E***, ***F***), 200 μm; ***C*** (for ***C***, ***D***), 100 μm. ac, Anterior commissure; opt, optic tract.

bouts was low in unlesioned cage exchange rats and immepip-treated rats, but it was similar to controls in cage exchange rats with IFC or LC lesions. The number of REM bouts was increased in CeA–BST-lesioned rats compared with controls, which might account for the recovery of the amount of REM sleep observed in this experimental group. Nevertheless, CeA–BST-lesioned rats also showed an increased average number of REM bouts per hour in the baseline during the light phase, which suggests that this increase might be a consequence of the lesion rather than a stress-induced sleep change. These results suggest that the sleep fragmentation induced by stress seems to be caused by activation of the IFC and the arousal system (LC and TMN), and not the CeA–BST.

Late period of sleep disturbances (fifth and sixth hours after cage exchange)

During this period, all treatments restored more or less the normal amounts of wake and nREM sleep, so they were similar to controls (Fig. 10*B*,*C*), but REM sleep was fully restored only in rats with CeA–BST lesions and, to a lesser extent, with IFC lesions (Fig. 10*D*). These results suggest that all brain regions lesioned or inhibited seem to contribute to the nREM and wake perturbations induced by stress, suggesting high redundancy in the circuitry, whereas REM sleep disruption depends mainly on the activity of the CeA–BST and perhaps also the IFC. The percentages of wake, nREM, and REM at each time point (by hour) for all treatments are provided in Figure 12.

To summarize, difficulties falling asleep after cage exchange seem to be mainly mediated by the CeA–BST, and to a lesser extent by the arousal system (LC and TMN), whereas sleep fragmentation seems to be caused by activation of the IFC and the LC and TMN, but not the CeA–BST. All these brain regions seem to contribute to the nREM and wake perturbations induced by stress, whereas REM sleep disruption depends mainly on the activity of the CeA–BST.

Alterations of Fos expression in selected brain structures

We examined the Fos expression qualitatively throughout the brain in each of the lesion groups. In addition, we quantified the effects of the brain lesions and immepip treatment on Fos expression in a subset of sleep-promoting areas, limbic regions, and the arousal system (Table 2) 5.5 h after cage exchange. Total Fos counts for each area in all treatments are provided in Figure 13.

In general, Fos expression in the brains of rats with IFC lesions killed 5.5 h after cage exchange were more similar to those from unlesioned cage exchange rats than to controls. Nevertheless, there were several differences. Expression of Fos in the cerebral cortex was generally intermediate between that of controls and cage exchange animals, with the exception of piriform and endopiriform cortices that showed high Fos signal, whereas Fos expression in the preoptic area, thalamus, and medial amygdala was similar to that observed in cage exchange rats. There was more Fos signal in the lateral septum, premammillary nucleus, hippocampus, DMH, vlPAG, and PPT (noncholinergic neurons) than in controls. Fos expression in the rest of the pons and brainstem was similar to controls. The most striking difference was that in the areas in which Fos expression was quantified (Fig. 13), with the sole exception of the CeA/BST, there was reduction of Fos to levels similar to that seen in control animals. In contrast,

Fos expression in the CeA/BST remained at levels similar to unlesioned cage exchange rats.

The entire brains of rats with LC lesions showed less Fos expression than those from IFC-lesioned rats and cage exchange rats; indeed, they resembled control more than cage exchange rats. There was almost no Fos expression in the cortex, with the exception of small numbers of Fos-immunoreactive neurons in the cingulate and motor areas. The paraventricular thalamic nucleus was the only thalamic area that showed some Fos. There were high levels of Fos expression in the preoptic area, whereas lower Fos expression was observed in the hippocampus, medial amygdala, LH, DMH, and LDT (noncholinergic neurons). Conversely, there was high Fos expression in the vlPAG and PPT. In general, the brainstem showed less Fos than in controls and unlesioned cage exchange rats. In areas in which Fos expression was quantified (Fig. 13), LC-lesioned rats showed decreased Fos expression in the CeA and BST, similar to control levels, whereas Fos in the IFC and TMN was decreased but not to the levels seen in clean cage controls.

Brains from rats treated with immepip showed scattered Fos-positive neurons in the cortex, similar to controls and LC-lesioned rats, but the thalamus had as high Fos expression as unlesioned cage exchange rats. There was more Fos expression in the preoptic area (especially in the parastrial nucleus) and the hypothalamus in general than in the rest of the groups. The hippocampus and premammillary and supramammillary nuclei had little Fos, whereas the dorsal periaqueductal gray matter and vlPAG, PPT, and LDT showed high levels of expression. Fos in the brainstem was similar to controls and unlesioned cage exchange rats. Fos counts in selected areas (Fig. 13) shows that immepip treatment before cage exchange had no effect on Fos expression in the VLPOex, CeA, or BST; however, it decreased Fos to low levels in the IFC and LC, and totally abolished Fos expression in the TMN.

The brains of rats with CeA–BST lesions in general showed relatively low levels of Fos expression, similar to control animals. This was particularly true in the cell groups that were quantified (Fig. 13), in which levels of Fos expression were indistinguishable from control rats, as if the rats had not been exposed to cage exchange. On the other hand, scattered Fos-positive neurons were observed in the cingulate cortex in the brains of rats with CeA–BST lesions, and larger numbers of Fos immunoreactive neurons were seen in the piriform and dorsal endopiriform cortices, the medial amygdala, the paraventricular and rhomboid thalamic nuclei, and the hippocampus, as well as some hypothalamic nuclei, such as the zona incerta, LH, and dorsal hypothalamic area. In the pons and medulla, the vlPAG and LDT, as well as the medullary raphe

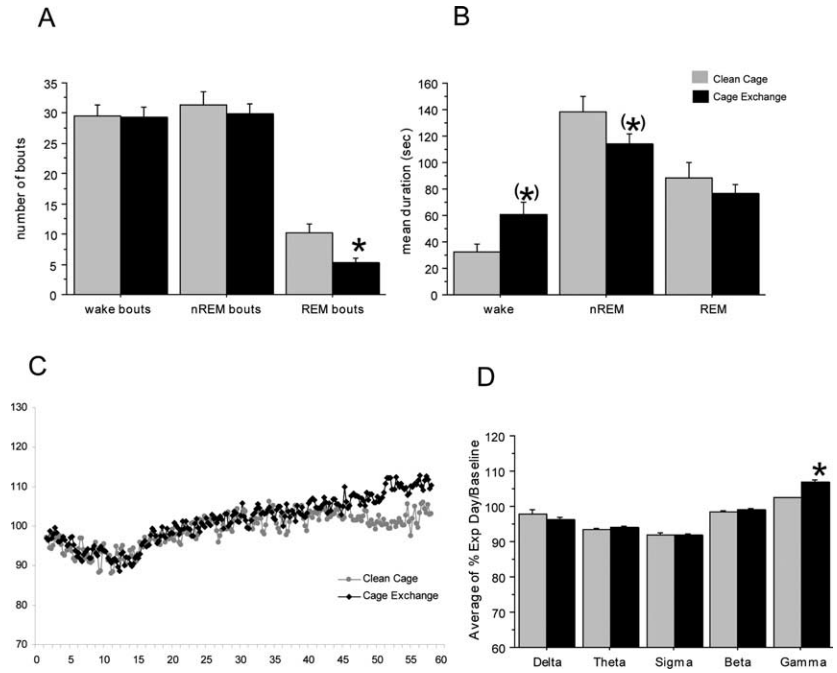

Figure 8. Microarchitecture of sleep during stress-induced insomnia (5–6 h after cage exchange). ***A***, When sleep was scored in 4 s epochs, only the number of REM bouts changed compared with scoring in 12 s epochs. ***B***, There was a trend (p between 0.05 and 0.08) to longer wake bouts and shorter nREM bouts in stressed rats, which accounts for the difference in percentage of wake and nREM sleep with respect to controls. These results ruled out rapid switching between wake and sleep states as the cause of simultaneous Fos expression in wake and sleep structures during stress-induced sleep disturbances. ***C***, ***D***, On the other hand, the ratio of the EEG power spectra during nREM sleep between the experimental day and the baseline showed an increase in high-frequency activity during the sleep-disturbed period from ~45 to 58 Hz, within the gamma band, which is usually associated with waking cortical activity in rats. Each point represents the average for each frequency at 0.25 Hz intervals ($n = 9$ and $n = 16$, for controls and stressed rats, respectively). In ***D***, the average power for each frequency band (delta = 1.5–4 Hz; theta = 4.25–8.75 Hz; sigma = 9–14 Hz; beta = 14.25–30 Hz; and gamma = 30.25–58 Hz) from controls and stressed rats were compared using unpaired t tests ($p < 0.05$). $^{*}p < 0.05$ between treatments at each time point; $^{(*)}p$ values of 0.05 and 0.08 for mean duration of wake bouts and nREM bouts, respectively, in ***B***. All values are the mean ± SEM.

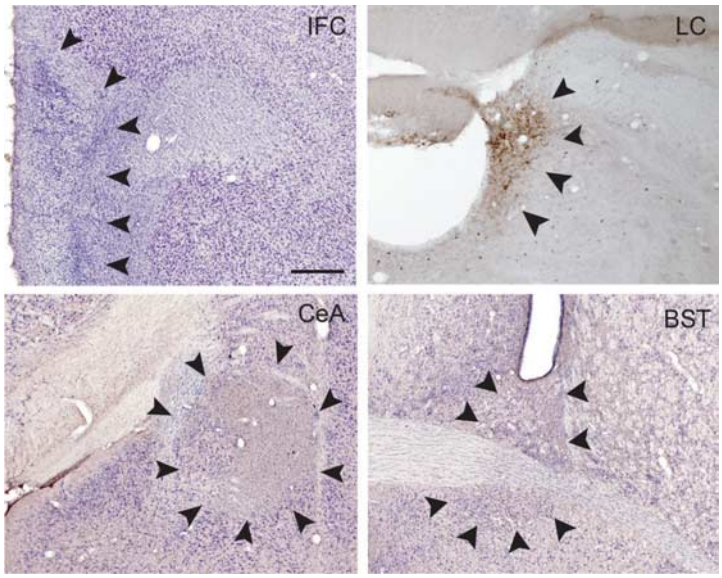

Figure 9. The extent of the lesions in the IFC, CeA, and BST are noted by arrowheads in Nissl-stained sections. The extent of the LC lesions was assessed by counting the remaining noradrenergic neurons in sections labeled for dopamine-β-hydroxylase (in the photomicrograph of the LC, there are 3 remaining immunoreactive neurons). Scale bar, 200 μm.

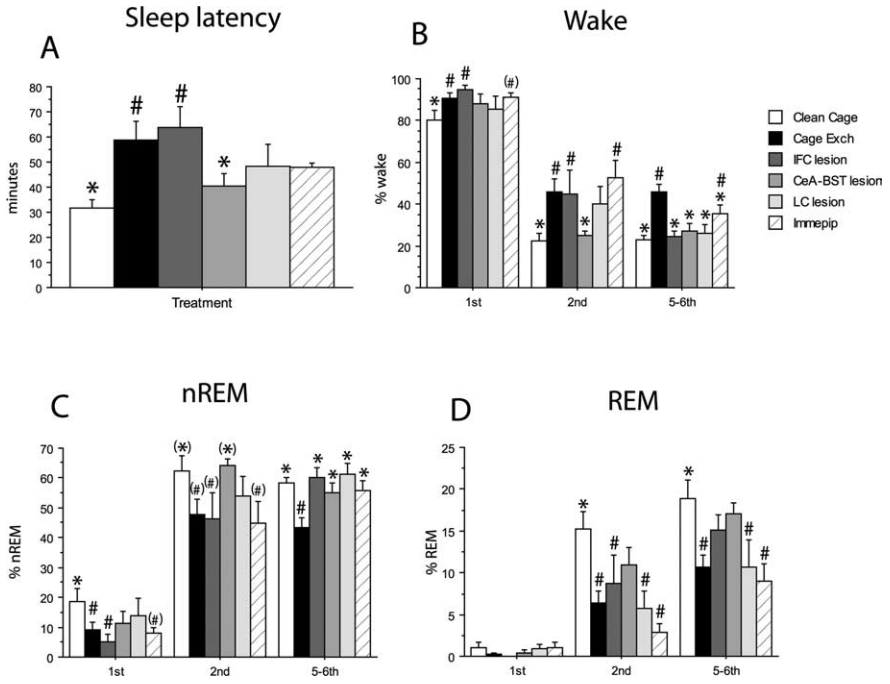

Figure 10. ***A***, Sleep latency in stressed rats is almost double than in controls. CeA–BST lesions restore sleep latency similar to control levels, whereas IFC lesions have no effect. LC lesions and immepip treatment before cage exchange decrease sleep latency ~10 min with respect to stressed rats, but this difference is not statistically significant. ***B***, ***C***, During the first hour after cage exchange, which corresponds to the primary stress response, almost all groups have increased wake (***B***) and decreased nREM (***C***) compared with clean cage controls. ***D***, REM levels are minimal in all groups, including controls. During the second hour, controls and CeA–BST-lesioned rats fall asleep similarly (***C***), whereas the other groups have increased wake (***B***) and decreased nREM (***C***) compared with controls. REM is decreased in all groups during this second hour. During the acute insomnia period (fifth and sixth hours after cage exchange), all treatments restore more or less the normal amounts of wake (***B***) and nREM (***C***), as in controls, but REM sleep is only recovered after CeA–BST lesions and to a lesser extent after IFC lesions (***D***). Percentages of wake, nREM, and REM at each time point for all treatments are provided in Figure 12. Data were analyzed by one-way ANOVA followed by Fisher's PLSD. $^{\#}$Significantly different from controls; *significantly different from cage exchange (Cage Exch) group. $^{\#,*}p < 0.05$; $^{(\#),(*)}p$ between 0.05 and 0.09. All values are the mean ± SEM.

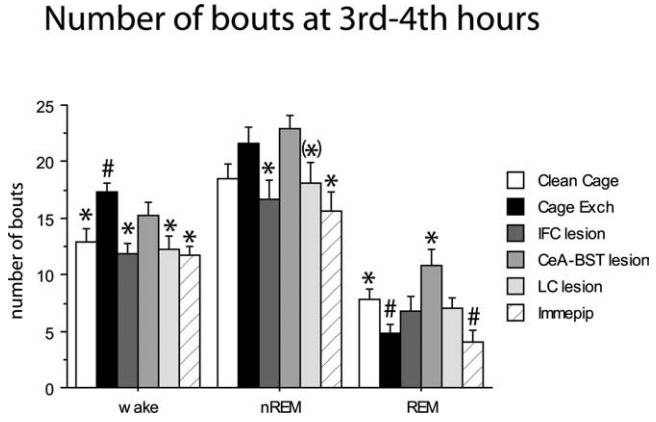

Figure 11. Number of bouts (wake, nREM, and REM) during the fragmentation period (third and fourth hours after cage exchange). The sleep fragmentation induced by stress seems to be caused by activation of the IFC and the arousal system (LC and TMN), but not the limbic system (CeA–BST). The results were analyzed using one-way ANOVA followed by Fisher's PLSD [each treatment compared with clean cage and cage exchange (Cage Exch) rats; for the sake of clarity, comparisons between treatments are not included]. $^{\#}$Significantly different from controls; *significantly different from cage exchange group. $^{\#,*}p < 0.05$; $^{(*)}p = 0.08$. All values are the mean ± SEM.

nuclei, showed high Fos expression. The pattern of Fos in the remainder of the brainstem was similar to controls.

In summary, the changes in Fos expression in the selected brain areas after cage exchange in rats with specific lesions or immepip treatment suggest a hierarchical relationship in the circuitry activated during stress-induced sleep disturbances (Fig. 14). In this model, the CeA and BST would be farthest upstream, activating the IFC and other components of the arousal system, including the LC, TMN, and non-orexin cells in the LH, because lesions of the CeA–BST eliminated nearly all the sleep disturbances induced by stress as well as the excessive Fos expression in the brain. The exception would be the sleep fragmentation seen in the third and fourth hours after cage exchange, which is presumably mediated mainly by the IFC, because IFC, but not CeA–BST, lesions eliminated sleep fragmentation, although IFC lesions could not abolish Fos in the CeA–BST. The LC was apparently needed to maintain full Fos activation of the CeA–BST, and contributed to activation of the IFC and TMN as well. H3 receptor activation by immepip, which inhibits the firing and expression of Fos by TMN neurons, mainly reduced Fos expression in the IFC and LC, suggesting that the TMN probably does not contribute to the activation of the CeA–BST.

Although Fos expression identifies neuronal groups that show increased activity associated with a particular stimulus, some neuronal groups that play an important role may not express Fos, whereas others that express Fos may be activated by the stimulus but not contribute to the ongoing physiological activity that is being assessed (in this case, sleep and wakefulness). It is therefore necessary to demonstrate the role of the activated circuitry by manipulating it and examining the effect on the behavioral or physiological output. We tried to do that by inactivating selected brain regions based on their increased Fos activity after cage exchange and on the fact that they were part of the circuitry that controls sleep–wakefulness or the circuitry involved in emotional stress responses. Nevertheless, the lesioned areas are not the only components of the brain circuitry responsible for the sleep disturbances induced by stress, which should be much more complex, as indicated by the number of regions that showed changes in Fos expression (Table 1). Considering that it is technically not feasible to lesion all these areas simultaneously, the proposed circuitry based on the results of the selected lesions should be viewed as an oversimplified and preliminary description, which begins to define relevant brain regions involved in the generation of the observed sleep disturbances.

Chemical phenotypes of neurons in the arousal and limbic systems activated during stress-induced sleep disturbances

All neurons expressing Fos in the LC after cage exchange were noradrenergic (i.e., tyrosine hydroxylase immunoreactive). Fos-positive neurons in the ventrolateral TMN cluster were most likely histaminergic, because nearly all neurons in this cell group are histaminergic, and their Fos expression was totally inhibited by immepip, which specifically acts on H3 inhibitory autoreceptors on histaminergic neurons. The vast majority of neurons that

express Fos in the LH were not orexin immunoreactive, but their chemical phenotype is unknown. We also tried to characterize Fos-positive neurons in the CeA and BST after cage exchange, and found that small numbers of them were immunoreactive for CRH, enkephalin, or neurotensin. Arginine vasopressin immunostaining did not label parvicellular neurons in the CeA and BST (although it stained the magnocellular neurons in the PVH and supraoptic nucleus). We were unable to label Fos-positive neurons in the TMN, CeA, BST, or LH with GABA or GAD67 antibodies, although the prevalence of large numbers of GABAergic neurons in these nuclei suggests that they may participate in this circuitry. A major limitation of this approach is that the numbers of immunoreactive neurons would probably have been greater if the rats had been pretreated with colchicine, but this treatment is not compatible with behavioral or Fos studies. Hence the double labeling we observed is certainly an underestimate of the participation of these neurotransmitter systems in our stress-induced insomnia model. Nevertheless, we were able to establish that in addition to noradrenergic neurons in the LC and histaminergic/GABAergic neurons in the TMN, CRH-, enkephalin-, and neurotensin-immunoreactive neurons in the CeA–BST are candidates for participating in the sleep disturbances induced by stress.

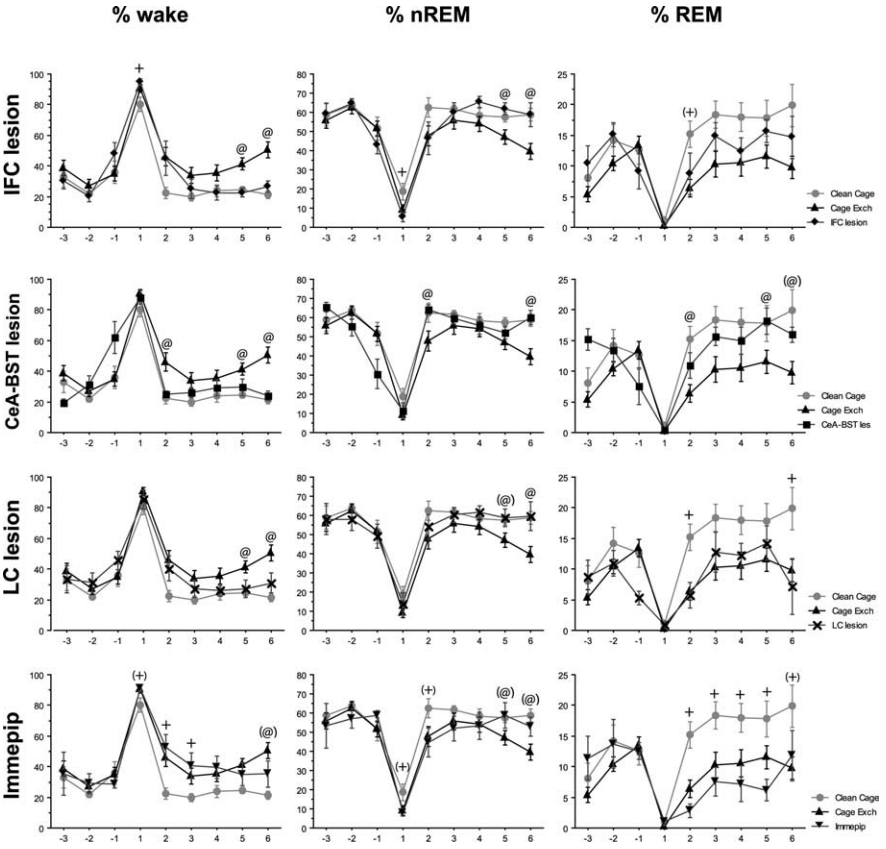

Figure 12. Percentages of wake, nREM and REM sleep at each time point for all treatments. These data are complementary to Figure 10. Comparisons were done with repeated-measures ANOVA followed by planned comparisons using Fisher's PLSD [each treatment compared with controls and cage exchange (Cage Exch)]. $^{+}$Significantly different from controls; $^{@}$significantly different from cage exchange group. $^{+,@}p < 0.05$; $^{(+),(@)}p$ between 0.05 and 0.09. Comparisons between controls and cage exchange rats are not included in these graphs (shown in Fig. 2). The *x*-axis is marked in hours before or after the cage exchange. All values are the mean ± SEM. les, Lesion.

High-frequency activity during nREM sleep in stress-induced sleep perturbations is associated with activation of the arousal system

We hypothesized that the high-frequency EEG activity observed in cage exchange rats during nREM sleep in the stress-induced insomnia period might be caused by activation of the arousal system because high-frequency activity is associated with cortical activation, and the cortex, which shows extensive Fos expression in these rats, receives dense projections from the LC and TMN that are also active. Moreover, inhibiting the LC and TMN with lesions or immepip treatment (respectively) substantially decreased Fos expression in the cortex, suggesting that these two nuclei might play an important role in cortical activation during stress-induced sleep disturbances. To test this hypothesis, we analyzed the EEG power spectrum during the stress-induced insomnia period in LC-lesioned rats and in rats treated with immepip, and compared this with the spectra of controls and cage exchange rats. LC lesions abolished the high-frequency activity observed during this period in the unlesioned cage exchange rats, and the power spectrum in the gamma band was similar to control rats (Fig. 15*A*). In addition, power in the theta and sigma bands was increased after LC lesions, but we do not know the functional implications of these changes during nREM sleep because these frequencies were not altered in unlesioned cage exchange rats. Immepip treatment decreased the high-frequency power (gamma band) to levels even lower than controls, and dramatically increased the delta power but had no effect on theta activity (Fig. 15*B*). This increase in delta power is not surprising because it has been previously reported after treatment with antihistaminergic sleep-inducing drugs (Lin et al., 1988; Tokunaga et al., 2007). In addition to inhibiting TMN neurons, immepip most likely inhibited histamine and norepinephrine release in the cortex by binding to H3 presynaptic receptors in TMN and LC axon terminals as these receptors also mediate presynaptic inhibition (Schlicker et al., 1994; Brown et al., 2001). This additional effect may explain the remarkable decrease in high-frequency power caused by immepip treatment. In agreement with this hypothesis, it has been reported that the LC has a high H3 receptor mRNA expression but a very low binding of selective radioligands (Pillot et al., 2002), suggesting that presynaptic rather than somatodendritic H3 heteroreceptors mediate the inhibition of norepinephrine release (Schlicker et al., 1994).

These results strongly suggest that the residual activity of the LC and the TMN during nREM sleep in cage exchange rats is important in mediating the high-frequency activity observed in the stress-induced insomnia period.

Discussion

We describe here a rat model of sleep perturbations induced by exposure to a species-specific psychological stressor (cage exchange) during the sleep phase. This experimental paradigm produces an initial period of acute stress with the classical indicators of autonomic and HPA axis activation. Although the animals remain in the dirty cages, these indicators are substantially atten-

Table 2. Different treatments (specific lesions and immepip injection) have different effects on Fos expression in sleep-promoting areas, limbic regions, and arousal system several hours after cage exchange exposure

	Sleep-promoting areas			Limbic system			Arousal system	
Treatment	MnPO	VLPOc	VLPOex	IFC	BST	CeA	TMN	LC
Wake	0	0	0	↑ ↑	↑	↑	↑ ↑ ↑	0
Clean cage	↑ ↑	↑ ↑	↑ ↑	↑	↑	↑	0	0
Cage Exc	↑ ↑	↑ ↑	↑ ↑ ↑	↑ ↑ ↑	↑ ↑	↑ ↑	↑ ↑ ↑	↑ ↑
IFC lesion	↑ ↑	↑ ↑	↑ ↑		↑ ↑	↑ ↑	0	0
CeA–BST lesion	↑ ↑	↑ ↑	↑ ↑	↑			0	0
LC lesion	↑ ↑	↑ ↑	↑ ↑ ↑	↑ ↑	↑	↑	↑	
Immepip	↑ ↑	↑ ↑	↑ ↑ ↑	↑	↑ ↑	↑ ↑	0	↑

IFC lesions generate a pattern of Fos similar to clean cage controls with the exception of the CeA and BST, which still remain activated. CeA–BST lesions totally restore Fos expression to control levels as if the rats were not exposed to stress. LC lesions do not restore Fos in the VLPOex, but do it in the CeA and BST, whereas Fos in the IFC and TMN is decreased to moderate and low levels, respectively. Immepip treatment has no effect on Fos expression in the VLPOex, CeA, and BST after cage exchange; however, it decreases Fos expression in the IFC and LC and totally abolishes it in the TMN. These results suggest the existence of a hierarchical circuitry underlying stress-induced acute insomnia, shown in Figure 14. (Total Fos counts for each area in all treatments are provided in Fig. 13.) Levels of Fos expression were as follows: 0, none; ↑, low; ↑ ↑, moderate; ↑ ↑ ↑, high. Exc, Exchange.

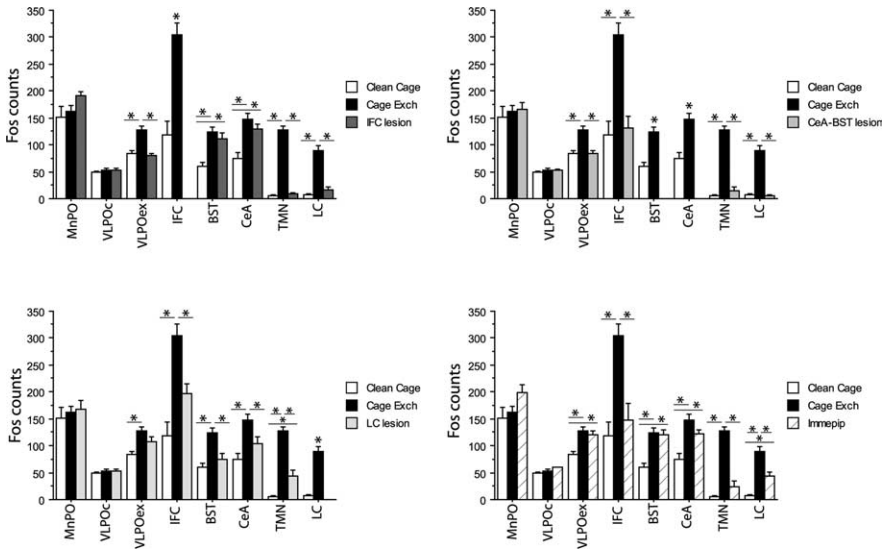

Figure 13. Total Fos counts in sleep-promoting areas, limbic regions, and arousal system for each treatment. These data are complementary to Table 2. Comparisons were done using one-way ANOVA followed by Fisher's PLSD for each planned comparison (*$p < 0.05$). All values are the mean ± SEM. Exch, Exchange.

uated 4–6 h after initial exposure, when the rats show a pattern of sleep loss and fragmentation resembling that observed in humans with acute insomnia after a stressful situation. In humans, the sleep impairment can be mediated by an internal psychological response when the external stressful stimulus is no longer present. To mimic this, we place the rats in a situation in which the psychological stress is generated by the social context in which they find themselves, as the olfactory cues are not novel. Under these conditions, we distinguish the late sleep disturbance period, in which rats sleep 25–30% less than controls, from the initial acute stress phase that induces not only robust activation of the PVH and orexin neurons but also sustained wakefulness (sleep deprivation, not insomnia). We therefore chose to study this late insomnia period, because it resembles the sleep disturbances induced by stress in humans and can be distinguished from the acute stress response.

The specific time frame of the late sleep disturbance period permitted us to examine the Fos expression in the brain to determine the neural circuitry activated. We found a unique pattern that includes coactivation of specific cortical, limbic, and arousal structures, and also the sleep-promoting circuitry. The high levels of cortical activity during nREM sleep were associated with high-frequency EEG activity, which is characteristic of wakefulness, generating an intermediate state that differs from both normal sleep and wakefulness. We analyzed the effects of lesions or pharmacological inhibition of selected arousal and limbic regions to determine their involvement in the stress-induced sleep disturbances and to delineate a tentative neuroanatomic circuitry that might underlie it.

In our model, the CeA and BST appear to play a key role, because only lesions of these structures can restore both nREM and REM sleep. We hypothesize that the olfactory cues of a conspecific male are likely to enter the arousal system at the CeA, which receives afferents from adjacent amygdaloid nuclei (medial and cortical), which in turn receive extensive input from the accessory olfactory system that relays information concerned with pheromones in rodents and is very important in social interactions (Lehman and Winans, 1982).

The CeA and BST both provide inputs to structures important in autonomic arousal (Saper, 2005) and to distal dendrites of LC neurons (Van Bockstaele et al., 1999) and probably of TMN neurons (Ericson et al., 1991). These latter nuclei might be partly responsible for decreasing nREM sleep in our model, as their inactivation restored it, but not for decreasing REM sleep. Although the LC is thought to decrease REM sleep under normal or stressful conditions (Liu et al., 2003), LC lesions were not sufficient to restore REM sleep after cage exchange. Only CeA–BST lesions restored REM sleep, suggesting that the limbic system modulates REM sleep not only via LC activation but also through other regions that receive direct projections from the CeA–BST (Dong et al., 2001). The cortical activation in our model is most likely caused by the LC and TMN because inhibition of these areas substantially diminishes cortical Fos expression and eliminates the high-frequency activity during nREM sleep (Fig. 15). The cortical activation may generate cognitive inputs that feed back on the limbic and arousal systems, perpetuating the situation by keeping them engaged.

The activation of sleep-promoting areas during stress-induced insomnia is surprising. The MnPO activation is in agreement with the increased Fos observed in this nucleus during accumulation of sleep pressure (Gvilia et al., 2006). However, previous models of sleep–wake control have proposed that the reciprocal inhibitory innervation between the VLPO, whose neu-

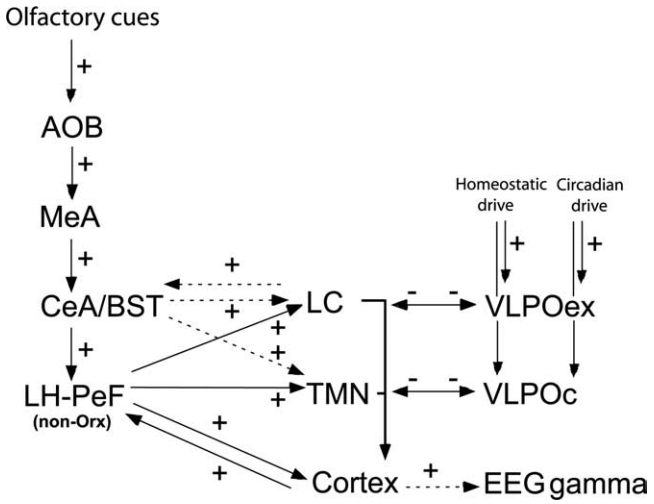

Figure 14. Simplified putative circuitry involved in stress-induced acute insomnia based on the results (sleep and Fos) of specific lesions and immepip treatment before stress exposure and on anatomical connections described in previous literature. The olfactory signals of a competing male rat are conveyed to the CeA–BST via the accessory olfactory bulb (AOB) and the medial amygdala (MeA). The CeA–BST, which projects densely to the lateral hypothalamus–perifornical area (LH–PeF), activates mainly nonorexin (non-Orx) neurons in this area. In addition, the LC and the TMN receive moderate and dense projections from the CeA–BST and the LH–PeF, respectively, which most likely causes the activation of these arousal regions during stress-induced insomnia. The cortex, which receives dense projections from the arousal system and the LH–PeF, becomes highly activated; this high cortical activity is associated with gamma activity during nREM in the insomnia period. The reciprocal inhibition between the VLPO (VLPOc and VLPOex) and the arousal system (LC and TMN) would ordinarily prevent coactivation. However, homeostatic and circadian sleep pressure keep the VLPO activated, whereas stress activates the arousal system, resulting in the unique pattern of Fos activation and EEG power spectrum seen during this acute insomnia period.

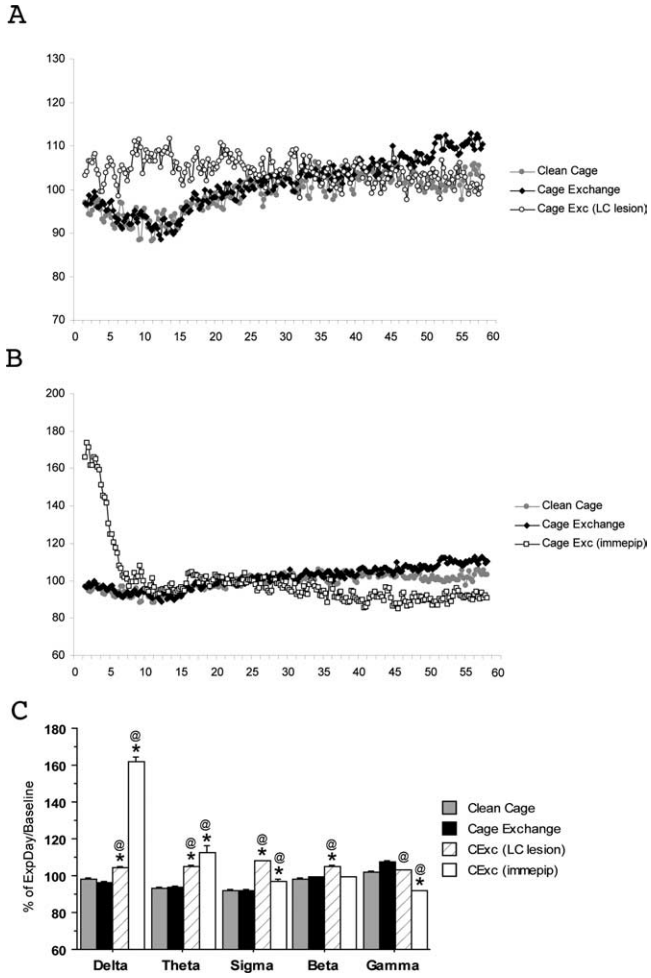

Figure 15. The increased high-frequency activity within the last portion of the gamma band (45–58 Hz) during nREM sleep observed in stressed rats during the acute insomnia period seems to be caused by activation of the LC and the TMN. ***A***, LC lesions abolished this high-frequency activity, and the power spectrum of the gamma band was similar to clean cage controls. LC lesions also increased theta (4.5–8.5 Hz) and sigma (9–14 Hz) power. ***B***, Immepip treatment, which inhibits the TMN, decreased the power along the whole gamma band (30–58 Hz) to lower levels than controls, and also increased delta power. In ***A*** and ***B***, each point represents the average of the ratio of power spectra during nREM sleep between the experimental day and the baseline for each frequency at 0.25 Hz intervals ($n = 9$ for controls; $n = 16$ for cage exchange; $n = 8$ for LC lesions; $n = 6$ for immepip treatment). Exc, Exchange. ***C***, The averages for each frequency band (delta = 1.5–4 Hz; theta = 4.25–8.75 Hz; sigma = 9–14 Hz; beta = 14.25–30 Hz; and gamma = 30.25–58 Hz) from controls, cage exchange, LC-lesioned rats, and immepip-treated rats were compared using one-way ANOVA followed by Fisher's PLSD for pair comparisons (*significantly different with respect to clean cage controls, $p < 0.05$; @significantly different with respect to cage exchange rats, $p < 0.05$). CExc, Cage exchange.

rons are activated during sleep, and the arousal system provides the conditions for a flip-flop switch, which imparts the property of rapid and complete transitions between sleep and wakefulness (McGinty and Szymusiak, 2000; Saper et al., 2001). We hypothesize that during insomnia the VLPO is fully activated as a result of both homeostatic and circadian pressure, but it is unable to turn off the arousal system because that is being excited intensely by the limbic system. Simultaneously, the arousal system cannot turn off the VLPO because of the strong excitatory homeostatic and circadian inputs. This results in a unique state in which the sleep circuitry shows Fos activation like that in a sleeping rat, but the Fos expression in the cortex and arousal system is similar to an awake rat (Fig. 5). An analogous process in insomniacs might explain the "sleep state misperception" reported in patients tested in sleep laboratories, who insist that they have been awake most of the night while the EEG shows mainly periods of nREM sleep.

The circuitry identified here differs from that engaged in another proposed model, in which animals are allowed to sleep in an environment where they previously have received electrical shocks (Pawlyk et al., 2005). This model, which mainly decreases REM sleep in the first 2 h, engages fear circuitry in the basal and lateral amygdala, LC, and dorsal raphe nucleus (Liu et al., 2003), but not in the TMN and CeA. Thus, different stressors may activate distinct neuronal circuitries and generate different patterns of sleep disturbances. It has been proposed that this fear conditioning-based model may reproduce PTSD, whereas we designed our model to mimic what might be experienced by humans during acute stress-induced insomnia.

Other models of insomnia involving lesions of the VLPO (Lu et al., 2000) or the midbrain dopaminergic neurons (Gerashchenko et al., 2006) may replicate conditions seen in neurodegenerative disorders but not those in stress-induced insomnia. Similarly, pharmacological models of insomnia, such as treatment with para-chloro-phenylalanine (Borbély et al., 1981) or caffeine (Paterson et al., 2007), do not mimic the sleep patterns observed in stress-induced insomnia. Other behavioral models of insomnia, such as having the rats sleeping on a grid over water (Shinomiya et al., 2003), essentially provide a continuous external stressor that generates partial sleep deprivation rather than insomnia induced by internally generated psychological stress. Hence, our model seems to reproduce conditions that are more comparable to stress-induced insomnia in humans.

Similar to humans who have experienced a stressful day

(Vgontzas and Kales, 1999), cage exchange rats have difficulty initiating sleep (increased sleep latency). Eventually, rats fall asleep because of the sleep pressure, as insomniacs do, but have difficulty maintaining sleep (increased wake, decreased nREM, and increased fragmentation). However, the most striking similarity between our rats and insomniacs is that both have simultaneously high levels of delta power (Perlis et al., 2001a,b) and high-frequency EEG activity during nREM sleep, a sign of continued cortical activation despite EEG slow wave activity (Freedman, 1986; Merica and Gaillard, 1992; Lamarche and Ogilvie, 1997; Merica et al., 1998; Perlis et al., 2001a). Because high-frequency activity is associated with enhanced sensory and cognitive processing, it has been proposed that the inability to disengage cognitive processes during nREM sleep may blur the distinction between sleep and wakefulness, causing sleep state misperception, which is correlated with increased high-frequency activity (Perlis et al., 2001b).

The pattern of Fos in our rats is also similar to the results of positron emission tomographic (PET) studies in primary insomniacs (Nofzinger et al., 2004). Compared with controls, insomniacs showed a smaller decline in glucose metabolism during the transition from wake to sleep in the arousal system, hypothalamus, cingulate and insular cortices, amygdala, hippocampus, and medial prefrontal cortex, demonstrating a failure of these areas to decline in activity during insomnia. The similarity of these findings with the regions showing increased Fos expression in our rats is remarkable because in both cases there is anomalous residual activation of the arousal and limbic systems during sleep. The preoptic sleep-promoting areas are too small to be distinguished in PET studies, but presumably they are active in insomniacs based on their relatively normal levels of EEG delta power.

Our results fit well with the conceptual models of primary insomnia as a disorder of hyperarousal (both physiologic and cognitive) (Morin, 1993; Bonnet and Arand, 1997; Perlis et al., 1997; Richardson and Roth, 2001; Nofzinger et al., 2004) or a disorder of sleep engagement caused by the inability to inhibit wakefulness rather than the inability to sleep (Espie, 2002). Moreover, our results provide a structural basis for the neuronal transition probability model, which proposes that in primary insomnia a failure in the coordination of neuronal groups in different activity modes could result in an intermediate state in which the dominant mode is sleep but with wake-related neuronal groups still active (Merica and Fortune, 1997; Perlis et al., 2001b).

Besides its limitations, the cage exchange model provides substantial behavioral and electrophysiological similarities with stress-induced insomnia in humans and suggests that the target for a more specific pharmacological treatment of insomnia might not be the sleep circuitry, which is fully active, but the arousal system or the upstream limbic system.

References

Alheid GF, Beltramino CA, De Olmos JS, Forbes MS, Swanson DJ, Heimer L (1998) The neuronal organization of the supracapsular part of the stria terminalis in the rat: the dorsal component of the extended amygdala. Neuroscience 84:967–996.

Arborelius L, Owens MJ, Plotsky PM, Nemeroff CB (1999) The role of corticotropin-releasing factor in depression and anxiety disorders. J Endocrinol 160:1–12.

Armstrong DM, Saper CB, Levey AI, Wainer BH, Terry RD (1983) Distribution of cholinergic neurons in rat brain: demonstrated by the immunocytochemical localization of choline acetyltransferase. J Comp Neurol 216:53–68.

Blanco-Centurion C, Gerashchenko D, Shiromani PJ (2007) Effects of saporin-induced lesions of three arousal populations on daily levels of sleep and wake. J Neurosci 27:14041–14048.

Bonnet MH, Arand DL (1997) Hyperarousal and insomnia. Sleep Med Rev 1:97–108.

Bonnet MH, Webb WB (1976) Effect of two experimental sets on sleep structure. Percept Mot Skills 42:343–350.

Borbély AA, Neuhaus HU, Tobler I (1981) Effect of p-chlorophenylalanine and tryptophan on sleep, EEG and motor activity in the rat. Behav Brain Res 2:1–22.

Bouyer JJ, Vallée M, Deminière JM, Le Moal M, Mayo W (1998) Reaction of sleep-wakefulness cycle to stress is related to differences in hypothalamo-pituitary-adrenal axis reactivity in rat. Brain Res 804:114–124.

Brown RE, Stevens DR, Haas HL (2001) The physiology of brain histamine. Prog Neurobiol 63:637–672.

Chemelli RM, Willie JT, Sinton CM, Elmquist JK, Scammell T, Lee C, Richardson JA, Williams SC, Xiong Y, Kisanuki Y, Fitch TE, Nakazato M, Hammer RE, Saper CB, Yanagisawa M (1999) Narcolepsy in orexin knockout mice: molecular genetics of sleep regulation. Cell 98:437–451.

Dalley JW, Cardinal RN, Robbins TW (2004) Prefrontal executive and cognitive functions in rodents: neural and neurochemical substrates. Neurosci Biobehav Rev 28:771–784.

Datiche F, Luppi PH, Cattarelli M (1995) Serotonergic and non-serotonergic projections from the raphe nuclei to the piriform cortex in the rat: a cholera toxin B subunit (CTb) and 5-HT immunohistochemical study. Brain Res 671:27–37.

Davis M, Shi C (1999) The extended amygdala: are the central nucleus of the amygdala and the bed nucleus of the stria terminalis differentially involved in fear versus anxiety? Ann N Y Acad Sci 877:281–291.

Dong HW, Petrovich GD, Watts AG, Swanson LW (2001) Basic organization of projections from the oval and fusiform nuclei of the bed nuclei of the stria terminalis in adult rat brain. J Comp Neurol 436:430–455.

Ericson H, Blomqvist A, Köhler C (1991) Origin of neuronal inputs to the region of the tuberomammillary nucleus of the rat brain. J Comp Neurol 311:45–64.

Espie CA (2002) Insomnia: conceptual issues in the development, persistence, and treatment of sleep disorder in adults. Annu Rev Psychol 53:215–243.

Estabrooke IV, McCarthy MT, Ko E, Chou TC, Chemelli RM, Yanagisawa M, Saper CB, Scammell TE (2001) Fos expression in orexin neurons varies with behavioral state. J Neurosci 21:1656–1662.

Freedman RR (1986) EEG power spectra in sleep-onset insomnia. Electroencephalogr Clin Neurophysiol 63:408–413.

Gaus SE, Strecker RE, Tate BA, Parker RA, Saper CB (2002) Ventrolateral preoptic nucleus contains sleep-active, galaninergic neurons in multiple mammalian species. Neuroscience 115:285–294.

Gerashchenko D, Blanco-Centurion CA, Miller JD, Shiromani PJ (2006) Insomnia following hypocretin2-saporin lesions of the substantia nigra. Neuroscience 137:29–36.

Gvilia I, Xu F, McGinty D, Szymusiak R (2006) Homeostatic regulation of sleep: a role for preoptic area neurons. J Neurosci 26:9426–9433.

Hughes J, Kosterlitz HW, Smith TW (1977) The distribution of methionine-enkephalin and leucine-enkephalin in the brain and peripheral tissues. Br J Pharmacol 61:639–647.

Ida T, Nakahara K, Murakami T, Hanada R, Nakazato M, Murakami N (2000) Possible involvement of orexin in the stress reaction in rats. Biochem Biophys Res Commun 270:318–323.

Jansen FP, Mochizuki T, Yamamoto Y, Timmerman H, Yamatodani A (1998) In vivo modulation of rat hypothalamic histamine release by the histamine H3 receptor ligands, immepip and clobenpropit. Effects of intrahypothalamic and peripheral application. Eur J Pharmacol 362:149–155.

Ko EM, Estabrooke IV, McCarthy M, Scammell TE (2003) Wake-related activity of tuberomammillary neurons in rats. Brain Res 992:220–226.

Kuru M, Ueta Y, Serino R, Nakazato M, Yamamoto Y, Shibuya I, Yamashita H (2000) Centrally administered orexin/hypocretin activates HPA axis in rats. Neuroreport 11:1977–1980.

Lamarche CH, Ogilvie RD (1997) Electrophysiological changes during the sleep onset period of psychophysiological insomniacs, psychiatric insomniacs, and normal sleepers. Sleep 20:724–733.

Lee MG, Hassani OK, Jones BE (2005) Discharge of identified orexin/hypocretin neurons across the sleep–waking cycle. J Neurosci 25:6716–6720.

Lehman MN, Winans SS (1982) Vomeronasal and olfactory pathways to the amygdala controlling male hamster sexual behavior: autoradiographic and behavioral analyses. Brain Res 240:27–41.

Lin JS, Sakai K, Jouvet M (1988) Evidence for histaminergic arousal mechanisms in the hypothalamus of cat. Neuropharmacology 27:111–122.
Liu X, Tang X, Sanford LD (2003) Fear-conditioned suppression of REM sleep: relationship to Fos expression patterns in limbic and brainstem regions in BALB/cJ mice. Brain Res 991:1–17.
Lu J, Greco MA, Shiromani P, Saper CB (2000) Effect of lesions of the ventrolateral preoptic nucleus on NREM and REM sleep. J Neurosci 20:3830–3842.
Lu J, Sherman D, Devor M, Saper CB (2006) A putative flip-flop switch for control of REM sleep. Nature 441:589–594.
Maloney KJ, Cape EG, Gotman J, Jones BE (1997) High-frequency gamma electroencephalogram activity in association with sleep-wake states and spontaneous behaviors in the rat. Neuroscience 76:541–555.
McGinty D, Szymusiak R (2000) The sleep-wake switch: a neuronal alarm clock. Nat Med 6:510–511.
Merica H, Fortune RD (1997) A neuronal transition probability model for the evolution of power in the sigma and delta frequency bands of sleep EEG. Physiol Behav 62:585–589.
Merica H, Gaillard JM (1992) The EEG of the sleep onset period in insomnia: a discriminant analysis. Physiol Behav 52:199–204.
Merica H, Blois R, Gaillard JM (1998) Spectral characteristics of sleep EEG in chronic insomnia. Eur J Neurosci 10:1826–1834.
Mileykovskiy BY, Kiyashchenko LI, Siegel JM (2005) Behavioral correlates of activity in identified hypocretin/orexin neurons. Neuron 46:787–798.
Moga MM, Saper CB, Gray TS (1989) Bed nucleus of the stria terminalis: cytoarchitecture, immunohistochemistry, and projection to the parabrachial nucleus in the rat. J Comp Neurol 283:315–332.
Morin CA (1993) Insomnia: psychological assessment and management. New York: Guilford.
Nofzinger EA, Buysse DJ, Germain A, Price JC, Miewald JM, Kupfer DJ (2004) Functional neuroimaging evidence for hyperarousal in insomnia. Am J Psychiatry 161:2126–2128.
Nowell PD, Buysse DJ, Reynolds CF 3rd, Hauri PJ, Roth T, Stepanski EJ, Thorpy MJ, Bixler E, Kales A, Manfredi RL, Vgontzas AN, Stapf DM, Houck PR, Kupfer DJ (1997) Clinical factors contributing to the differential diagnosis of primary insomnia and insomnia related to mental disorders. Am J Psychiatry 154:1412–1416.
Oka T, Oka K, Hori T (2001) Mechanisms and mediators of psychological stress-induced rise in core temperature. Psychosom Med 63:476–486.
Pagel JF, Parnes BL (2001) Medications for the treatment of sleep disorders: an overview. Prim Care Companion J Clin Psychiatry 3:118–125.
Paterson LM, Wilson SJ, Nutt DJ, Hutson PH, Ivarsson M (2007) A translational, caffeine-induced model of onset insomnia in rats and healthy volunteers. Psychopharmacology 191:943–950.
Pawlyk AC, Jha SK, Brennan FX, Morrison AR, Ross RJ (2005) A rodent model of sleep disturbances in posttraumatic stress disorder: the role of context after fear conditioning. Biol Psychiatry 57:268–277.
Pawlyk AC, Morrison AR, Ross RJ, Brennan FX (2008) Stress-induced changes in sleep in rodents: models and mechanisms. Neurosci Biobehav Rev 32:99–117.
Paxinos G, Watson C (1998) The rat brain in stereotaxic coordinates, Ed 4. San Diego: Academic.
Perlis ML, Giles DE, Mendelson WB, Bootzin RR, Wyatt JK (1997) Psychophysiological insomnia: the behavioural model and a neurocognitive perspective. J Sleep Res 6:179–188.
Perlis ML, Smith MT, Andrews PJ, Orff H, Giles DE (2001a) Beta/Gamma EEG activity in patients with primary and secondary insomnia and good sleeper controls. Sleep 24:110–117.
Perlis ML, Kehr EL, Smith MT, Andrews PJ, Orff H, Giles DE (2001b) Temporal and stagewise distribution of high frequency EEG activity in patients with primary and secondary insomnia and in good sleeper controls. J Sleep Res 10:93–104.
Phelps EA, LeDoux JE (2005) Contributions of the amygdala to emotion processing: from animal models to human behavior. Neuron 48:175–187.
Pillot C, Heron A, Cochois V, Tardivel-Lacombe J, Ligneau X, Schwartz JC, Arrang JM (2002) A detailed mapping of the histamine H(3) receptor and its gene transcripts in rat brain. Neuroscience 114:173–193.
Richardson GS, Roth T (2001) Future directions in the management of insomnia. J Clin Psychiatry 62 [Suppl 10]:39–45.
Ross RJ, Ball WA, Sullivan KA, Caroff SN (1989) Sleep disturbance as the hallmark of posttraumatic stress disorder. Am J Psychiatry 146:697–707.
Roth T, Roehrs T (2003) Insomnia: epidemiology, characteristics, and consequences. Clin Cornerstone 5:5–15.
Sakamoto F, Yamada S, Ueta Y (2004) Centrally administered orexin-A activates corticotropin-releasing factor-containing neurons in the hypothalamic paraventricular nucleus and central amygdaloid nucleus of rats: possible involvement of central orexins on stress-activated central CRF neurons. Regul Pept 118:183–191.
Saper CB (2005) Central autonomic system. In: The rat nervous system, Ed 2 (Paxinos G, ed), pp 107–128. San Diego: Academic.
Saper CB, Chou TC, Scammell TE (2001) The sleep switch: hypothalamic control of sleep and wakefulness. Trends Neurosci 24:726–731.
Sarkisova KIu, Kolomeĭtseva IA (1993) Individual differences in the reactions to acute stress related to behavioral type. Resistance (predisposition) to behavioral and sleep disorders (in Russian). Biull Eksp Biol Med 116:130–132.
Sarrais F, de Castro Manglano P (2007) The insomnia (in Spanish). An Sist Sanit Navar 30 [Suppl 1]:121–134.
Schlicker E, Malinowska B, Kathmann M, Göthert M (1994) Modulation of neurotransmitter release via histamine H3 heteroreceptors. Fundam Clin Pharmacol 8:128–137.
Shinomiya K, Shigemoto Y, Okuma C, Mio M, Kamei C (2003) Effects of short-acting hypnotics on sleep latency in rats placed on grid suspended over water. Eur J Pharmacol 460:139–144.
Sullivan RM, Gratton A (2002) Prefrontal cortical regulation of hypothalamic-pituitary-adrenal function in the rat and implications for psychopathology: side matters. Psychoneuroendocrinology 27:99–114.
Swanson LW (1976) The locus coeruleus: a cytoarchitectonic, Golgi and immunohistochemical study in the albino rat. Brain Res 110:39–56.
Takada M (1990) The A11 catecholamine cell group: another origin of the dopaminergic innervation of the amygdala. Neurosci Lett 118:132–135.
Tokunaga S, Takeda Y, Shinomiya K, Hirase M, Kamei C (2007) Effects of some H1-antagonists on the sleep-wake cycle in sleep-disturbed rats. J Pharmacol Sci 103:201–206.
Toussaint M, Luthringer R, Schaltenbrand N, Nicolas A, Jacqmin A, Carelli G, Gresser J, Muzet A, Macher JP (1997) Changes in EEG power density during sleep laboratory adaptation. Sleep 20:1201–1207.
Van Bockstaele EJ, Peoples J, Valentino RJ (1999) A. E. Bennett Research Award. Anatomic basis for differential regulation of the rostrolateral perilocus coeruleus region by limbic afferents. Biol Psychiatry 46:1352–1363.
Vgontzas AN, Kales A (1999) Sleep and its disorders. Annu Rev Med 50:387–400.
Vgontzas AN, Tsigos C, Bixler EO, Stratakis CA, Zachman K, Kales A, Vela-Bueno A, Chrousos GP (1998) Chronic insomnia and activity of the stress system: a preliminary study. J Psychosom Res 45:21–31.
Winsky-Sommerer R, Yamanaka A, Diano S, Borok E, Roberts AJ, Sakurai T, Kilduff TS, Horvath TL, de Lecea L (2004) Interaction between the corticotropin-releasing factor system and hypocretins (orexins): a novel circuit mediating stress response. J Neurosci 24:11439–11448.